For Reference

NOT TO BE TAKEN FROM THIS ROOM

For Reference

NOT TO BE TAKEN FROM THIS ROOM

Ex libris
universitatis
albertaensis

University of Alberta
Printing Department

Digitized by the Internet Archive
in 2019 with funding from
University of Alberta Libraries

https://archive.org/details/Semeniuk1966

1966A
#156

THE UNIVERSITY OF ALBERTA

STABILITY OF CAMBERED BITRAPEZOIDAL PLATES

BY

ALEXANDER SEMENIUK, B.Sc. (Alberta)

A THESIS

SUBMITTED TO THE FACULTY OF GRADUATE STUDIES

IN PARTIAL FULFILMENT OF THE REQUIREMENTS FOR THE DEGREE

OF MASTER OF SCIENCE

.

DEPARTMENT OF MECHANICAL ENGINEERING

EDMONTON, ALBERTA

OCTOBER 1966

UNIVERSITY OF ALBERTA

FACULTY OF GRADUATE STUDIES

The undersigned certify that they have read, and recommend to the Faculty of Graduate Studies for acceptance, a thesis entitled "STABILITY OF CAMBERED BITRAPEZOIDAL PLATES" submitted by ALEXANDER SEMENIUK in partial fulfilment of the requirements for the degree of Master of Science.

ABSTRACT

Moment-curvature relationships have been developed for plates with various transverse cross sections by previous investigators. The main purpose of this thesis was to extend this work to include plates with cambered bitrapezoidal cross sections. Experimental results are presented showing good agreement between theory and experiment. The theory indicated that if the camber was increased beyond a critical value, the plates exhibited a bending instability for certain values of curvature. This instability characteristic was verified by experiment.

The theory presented was for a general cross section. By changing certain parameters the theory was shown to approach the linear theory for a flat plate with a rectangular cross section and it also approached the results obtained for a plate with a bitrapezoidal cross section with no camber.

ACKNOWLEDGMENTS

The author wishes to extend his appreciation to Dr. D. G. Bellow for his guidance and supervision of this thesis.

Thanks are also extended to the members of the Mechanical Engineering shop; particularly Ray Marak, who aided in the instrumentation; Staff of the University of Alberta Computing Centre, whose assistance proved very helpful; National Research Council for their Bursary, which made this thesis possible; and to my wife Vera and sister Jean for their patience and ability in typing the thesis.

TABLE OF CONTENTS

SECTION		PAGE
	INTRODUCTION	1
	CHAPTER I	
	THEORETICAL CONSIDERATION	
1.1	Historical Review	2
1.2	Development of Theory	4
1.3	Moment-Curvature Relationship	8
1.4	Discussion of Theoretical Results	13
1.5	Comparison of Theory to Previous Results	18
	CHAPTER II	
	EXPERIMENTAL APPARATUS	
2.1	Plates	22
2.2	Strain Gauges	24
2.3	Loading Apparatus	26
2.4	Measurement of Curvature	30
2.5	Testing Procedure	31
	CHAPTER III	
	EXPERIMENTAL AND THEORETICAL RESULTS	
3.1	Remarks on Experimental Results	32
3.2	Comparison Between Experimental and Theoretical Results	32
3.3	Discussion of Results	34
3.4	Concluding Remarks on Chapter III	42
	CHAPTER IV	
	CONCLUSIONS AND FURTHER PROBLEMS	
4.1	Conclusions	43
4.2	Problems for Further Study	43
	TABLE OF REFERENCES	44
	APPENDIX A	
	Computer Program to Evaluate Constants of Integration and Theoretical Moment-Curvature Relationships	45
	APPENDIX B	
	Computer Program For Evaluating Bending Moment and Longitudinal Curvature From Strain Gauge Readings	57

LIST OF FIGURES

FIG. NO.		PAGE
1.1	Flügge's Cross Section	3
1.2	Fung and Wittrick's Cross Section	3
1.3	Author's Cross Section	3
1.3A	Alternative Cross Section	3
1.4	Plate Element	5
1.5	General Cross Section	5
1.6	Plate Orientation	5
1.7	Plate Strip	9
1.8	Theoretical Moment-Curvature Relationships for Variation in k (concave side down)	14
1.9	Theoretical Moment-Curvature Relationships for Variation in k (concave side up)	15
1.10	Theoretical Moment-Curvature Relationships for Variation in c (concave side down)	16
1.11	Theoretical Moment-Curvature Relationships for Variation in c (concave side up)	17
1.12	Comparison of Theory With Previous Work for Bitrapezoidal Cross Section	20
1.13	Comparison With Linear Theory for a Rectangular Cross Section Plate	21
2.1	Cross Section of Plate I-A	23
2.2	Cross Section of Plate I-B	23
2.3	Cross Section of Plate I-C	23
2.4	Cross Section of Plate II-A	25
2.5	Cross Section of Plate II-B	25
2.6	Cross Section of Plate II-C	25
2.7	Measuring Stations for Plate I-A	27
2.8	Measuring Stations for Plates I-B and I-C	27
2.9	Measuring Stations for Plate II-A	28
2.10	Measuring Stations for Plates II-B and II-C	28
2.11	Photographic View of Loading Apparatus	29
3.1	Diagram for Obtaining Correction Moment	33
3.2	Comparison of Theoretical and Experimental Results for Plate I-A	35
3.3	Comparison of Theoretical and Experimental Results for Plate I-B	36
3.4	Comparison of Theoretical and Experimental Results for Plate I-C	37
3.5	Comparison of Theoretical and Experimental Results for Plate II-A	38
3.6	Comparison of Theoretical and Experimental Results for Plate II-B	39
3.7	Comparison of Theoretical and Experimental Results for Plate II-C	40

LIST OF SYMBOLS

x, y, z	-	rectangular co-ordinates
M_y, M_x	-	moment per unit distance acting on the plane perpendicular to y and x axis respectively
M_{xy}	-	twisting moment per unit distance
b	-	one-half plate width
t	-	total thickness of plate
t_o	-	one-half the thickness of the tapered portion of the plate
k	-	dimensionless parameter defining amount of camber (Fig. 1.5)
N_x, N_y	-	membrane forces per unit distance in x and y directions respectively
R_y	-	longitudinal radius of curvature
R_x	-	transverse radius of curvature
R	-	radius of curvature measured from neutral surface in the plate cross section
Q_x, Q_y	-	shearing forces per unit distance
θ	-	angle measurement
E	-	modulus of elasticity
μ	-	Poisson's ratio
w	-	deflection in z-direction of centre line of cross section from neutral surface
w_o	-	initial deflection of centre line of cross section from neutral surface
ζ	-	deflection in z-direction of centre line of cross section from neutral surface due to applied moments only
ζ_o	-	particular solution of governing differential equation
ζ^*	-	complimentary solution of governing differential equation
V_x	-	shearing force per unit distance on edge of plate
e	-	strain in μ-in./in.
e_B	-	double bending strain in μ-in./in. as obtained from strain indicator
I	-	moment of inertia about neutral surface
c	-	plate edge thickness

OTHER RELATIONSHIPS

$$w = w_o + \zeta$$

$$\rho = \frac{t}{t_o}$$

$$\xi = 1 - \frac{x}{b}$$

$$\lambda^4 = \frac{3b^4(1 - \mu^2)}{R^2 t_o^2}$$

$$t = 2t_o(1 - \frac{x}{b}) + c$$

$$\beta = \frac{c}{2t_o}$$

$$\gamma = \xi + \beta$$

$$\varepsilon = 2\lambda\beta^{\frac{1}{2}}$$

$$\alpha = 2\lambda(1 + \beta)^{\frac{1}{2}}$$

$$\eta = 2\lambda\gamma^{\frac{1}{2}}$$

Other symbols not defined here are defined when used.

INTRODUCTION

The governing equation for the moment-curvature relationship for a plate with a rectangular cross section can be written as

$M = -\frac{EI}{R}\left(\frac{1 - \bar{k}\mu^2}{1 - \mu^2}\right)$ where EI is the stiffness, R is the radius of curvature in the longitudinal direction, μ is Poisson's ratio and $\bar{k}$ is a parameter which depends on the ratio $\frac{d^2}{Rt}$ (d is the width and t is the thickness of the plate). For a beam $\bar{k} = 1$, and for a plate $\bar{k} = 0$ (i.e. a plate is one whose width is many times larger than its thickness). For beams and plates with rectangular cross sections there is a gradual transition in $\bar{k}$ from a value of one to zero as the width of the beam is increased while the thickness is held constant.

When plates with tapered cross sections are considered, the moment-curvature relationship becomes more complicated. The aim of this thesis was to investigate theoretically and experimentally the stability of plates with a general bitrapezoidal cross section and to show that with suitable parameter changes, the theory approached the results obtained by other investigators.

CHAPTER I

THEORETICAL CONSIDERATIONS

1.1 HISTORICAL REVIEW

The problem of finding a moment-curvature relationship for a flat plate with a rectangular cross section, with its longitudinal edges being free, was first investigated by Kelvin and Tait[1]* in 1879. Timoshenko[2] modified the form of Kelvin and Tait's equation by including the $\bar{k}$ term which accounted for the transition from a beam to a plate. In 1949, Flügge[3] obtained moment-curvature relationships for various forms of tapered cross sections. Some of the sections he considered were rectangular, double-wedge and certain bitrapezoidal cross sections. Flügge obtained his results by assuming a power series form of solution. Ashwell[4], in 1952, considered the bending instability of curved rectangular plates. Later, Ashwell[5] extended his work to include bending instability of slightly corrugated rectangular plates. Fung and Wittrick[6] in 1954, mentioned the problem of bending instability for plates with a double-wedge cross section, however, no theory was presented.

One of the cross sections considered by Flügge[3] had finite edge thickness but no camber (see Fig. 1.1). Fung and Wittrick[6] considered a cross section with infinitely thin edges including a camber as shown in Fig. 1.2. In the bending of plates with cross sections as shown in Fig. 1.3A, torsional instability develops. Goodier[7] discussed torsional instability in thin-walled, constant thickness, open section channels, however, this was beyond the scope of this thesis.

---

* Numbers in parenthesis refer to references at the end of thesis.

The theory developed in this thesis is for a tapered cross section having finite edge thickness and camber (Fig. 1.3) which does not exhibit torsional instability. By a change in sign for the parameter w_o, the theory may be applied to a plate with a cross section as shown in Fig. 1.3A. However, torsional instability is not taken into account in the analysis.

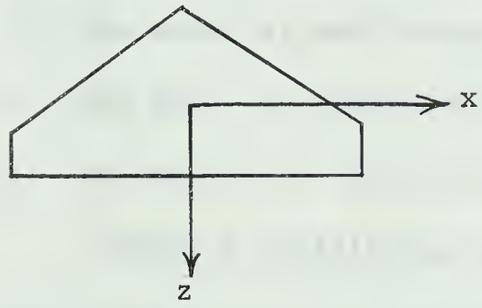

FIG. 1.1

FLÜGGE'S CROSS SECTION

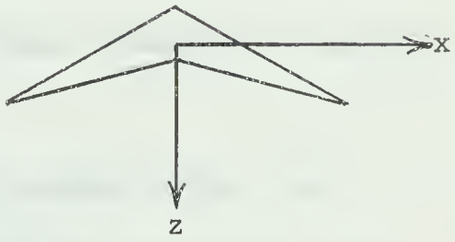

FIG. 1.2

FUNG AND WITTRICK'S CROSS SECTION

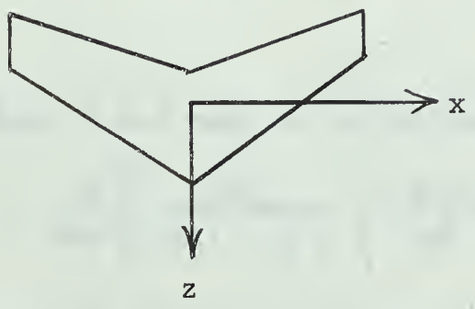

FIG. 1.3

AUTHOR'S CROSS SECTION

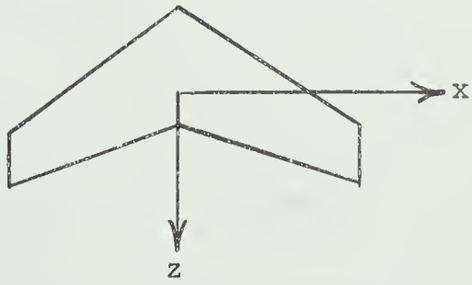

FIG. 1.3A

ALTERNATIVE CROSS SECTION

1.2 DEVELOPMENT OF THEORY

The governing differential equation was obtained by considering the equilibrium of a plate element as shown in Fig. 1.4. The general cross section considered is shown in Fig. 1.5 and the manner in which the plate was loaded is shown in Fig. 1.6.

The assumptions used in the development of the theory were as follows:

a) The behavior of the material under loading was perfectly elastic and obeyed Hooke's Law.

b) The material was homogeneous.

c) The slope of transverse deflection curve was small compared to unity.

d) The weight of the plate was zero.

Applying equilibrium conditions to the plate element (Fig. 1.4) and using geometrical and Hooke's Law relationships the following differential equation was obtained

$$\frac{d^2}{dx^2}\left[\frac{Et^3}{12(1-\mu^2)}\left(\frac{d^2w}{dx^2}+\frac{\mu}{R-w}\right)\right]+\frac{Ewt}{(R-w)^2}=0 \qquad 1.2\text{-}1$$

where the thickness t of the transverse section is

$$t = 2t_o\left(1-\frac{x}{b}\right)+c \qquad 1.2\text{-}2$$

for any positive x and c is the edge thickness. The transverse deflection w can be assumed to be small compared to R, hence

$$R - w \doteq R.$$

Eqn. 1.2-1 can now be written as

$$\frac{d^2}{dx^2}\left[\frac{Et^3}{12(1-\mu^2)}\left(\frac{d^2w}{dx^2}+\frac{\mu}{R}\right)\right]+\frac{Ewt}{R^2}=0. \qquad 1.2\text{-}3$$

Lamb[8] obtained a solution to the above equation for a plate of constant thickness t.

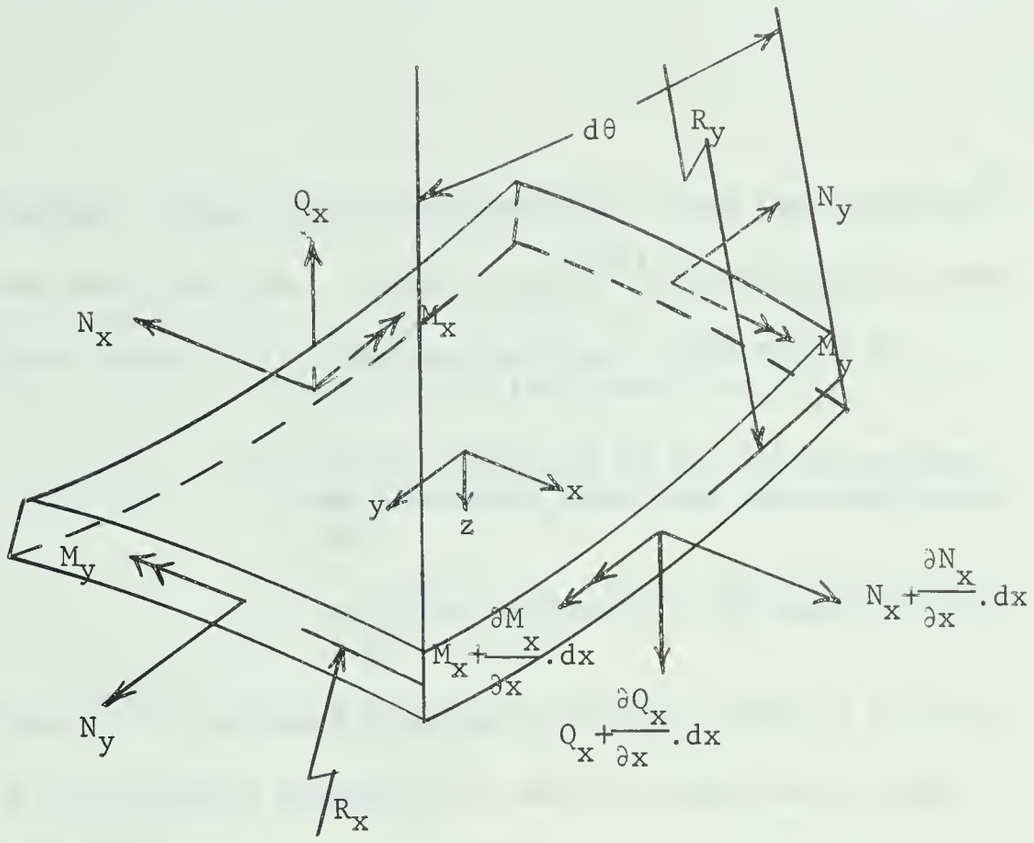

FIG. 1.4 PLATE ELEMENT

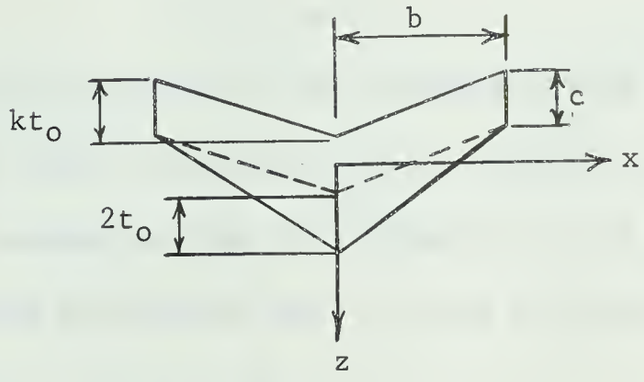

FIG. 1.5 GENERAL CROSS SECTION

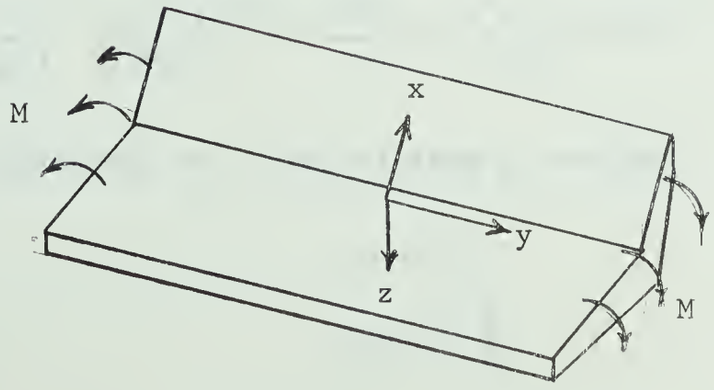

FIG. 1.6 PLATE ORIENTATION

Using von Kármán's large deflection equations, Fung and Wittrick[6] obtained the same result as Lamb. These authors[6] extended their work to include the case where: (a) the cross section of the plate had a variable thickness t(x),

(b) initial mid-line of the cross section was displaced from the centroidal axis, and

(c) the cross section had no edge thickness, (i.e. c = 0).

Bellow and Faulkner[9,10] extended Fung and Wittrick's work to a cross section (see Fig. 1.3A) which included (a) and (b) above and an edge thickness, i.e. c > 0.

To simplify calculations let

$$w = w_o + \zeta, \tag{1.2-4}$$

where w_o is the initial distortion of the mid-line of the cross section from the neutral axis, and ζ is the additional deflection due to the applied moments. By considering the first moment of area of the cross section (Fig. 1.5) about the neutral axis, it can be shown that

$$w_o = t_o(1 + k)\left[1 - \frac{x}{b} - \frac{\beta + 2/3}{2\beta + 1}\right] \tag{1.2-5}$$

where $\beta = \frac{c}{2t_o}$.

Since w_o is a linear function of x, Eqn. 1.2-3 becomes

$$\frac{d^2}{dx^2}\left(t^3 \frac{d^2\zeta}{dx^2}\right) + \frac{\mu}{R}\frac{d^2(t^3)}{dx^2} + \frac{12t(1 - \mu^2)(\zeta + w_o)}{R^2} = 0. \tag{1.2-6}$$

This can be transformed to a simpler form by setting

$$\rho = \frac{t}{t_o}$$

and

$$\xi = 1 - \frac{x}{b}$$

yielding

$$\frac{d^2}{d\xi^2}\left(\rho^3 \frac{d^2\zeta}{d\xi^2}\right) + \frac{\mu b^2}{R}\frac{d^2}{d\xi^2}(\rho^3) + 4\lambda^4\rho(\zeta + w_o) = 0 \qquad 1.2\text{-}7$$

where $\lambda^4 = \frac{3b^4(1 - \mu^2)}{R^2 t_o^2}$ and t_o is defined as one-half the thickness of the tapered portion of the plate (Fig. 1.5). Further simplifications were made by substituting

$$\gamma = \xi + \beta,$$

giving the final form of Eqn. 1.2-7 as

$$\frac{d^2}{d\gamma^2}\left(\gamma^3 \frac{d^2\zeta}{d\gamma^2}\right) + \frac{6\mu b^2\gamma}{R} + \lambda^4\gamma(\zeta + w_o) = 0. \qquad 1.2\text{-}8$$

In the solution of Eqn. 1.2-8 let ζ_o be the particular solution and ζ^* be the complimentary solution. Thus, ζ_o becomes

$$\zeta_o = - w_o - \frac{6\mu b^2}{\lambda^4 R}, \qquad 1.2\text{-}9$$

and the complimentary equation becomes

$$\frac{d^2}{d\gamma^2}\left(\gamma^3 \frac{d^2\zeta^*}{d\gamma^2}\right) + \lambda^4\gamma\zeta^* = 0. \qquad 1.2\text{-}10$$

Eqn. 1.2-10 is of the same form as obtained for the solution of a cylindrical tank with non-uniform wall thickness. Timoshenko[11] and Flügge[12] obtained the following solution to Eqn. 1.2-10:

$$\zeta^* = \frac{1}{\eta}\left[A\ \mathrm{ber}'\eta + B\ \mathrm{bei}'\eta + C\ \mathrm{ker}'\eta + D\ \mathrm{kei}'\eta\right] \qquad 1.2\text{-}11$$

where η is defined as

$$\eta = 2\lambda\gamma^{\frac{1}{2}}.$$

The complete solution may be written as

$$\zeta = \zeta_o + \zeta^*$$

or after substituting for ζ_o and ζ^*, ζ becomes

$$\zeta = \frac{1}{\eta}\,[A\ \mathrm{ber}'\eta + B\ \mathrm{bei}'\eta + C\ \mathrm{ker}'\eta + D\ \mathrm{kei}'\eta] - w_o - \frac{6\mu b^2}{\lambda^4 R} \qquad 1.2\text{-}12$$

where the prime denotes differentiation with respect to η.

The constants of integration A, B, C, and D can be solved from the following four conditions:

(a) $$M_x = \frac{-Et^3}{12(1-\mu^2)}\left[\frac{d^2w}{dx^2} + \frac{\mu}{R}\right]_{x=b} = 0,$$

(b) $$V_x = \left[Q_x + \frac{\partial}{\partial y}(M_{xy})\right]_{x=b} = 0$$

since $\left[M_{xy}\right]_{x=b} = 0$, (b) reduces to

$$\left[\frac{d^3w}{dx^3}\right]_{x=b} = 0\ .$$

(c) from the symmetry of the problem

$$\left[\frac{d\zeta}{dx}\right]_{x=0} = 0, \text{ and}$$

(d) $$\int_{-b}^{b} N_y\,dx = 0.$$

The above equations were transformed into non-dimensional form and the constants A, B, C, and D were solved using an IBM 7040/1401 digital computer.

1.3 MOMENT-CURVATURE RELATIONSHIP

By considering moment equilibrium of an elemental strip of width dx, the external moment dM applied to the transverse edge must balance the two internal moments $(M_y)dx$ and $(N_y w)dx$ (Fig. 1.7). Writing the equilibrium equation for Fig. 1.7

$$dM = (M_y)dx + (N_y w)dx$$

$$\text{or} \quad M = 2\int_{o}^{b} (M_y)\,dx + 2\int_{o}^{b} (N_y w)\,dx \qquad 1.3\text{-}1$$

noting that the cross section is symmetrical about the centre line. The internal moment $N_y w$, is the moment per unit width which is induced when the centre line of the cross section is displaced from the centroidal axis by an amount w.

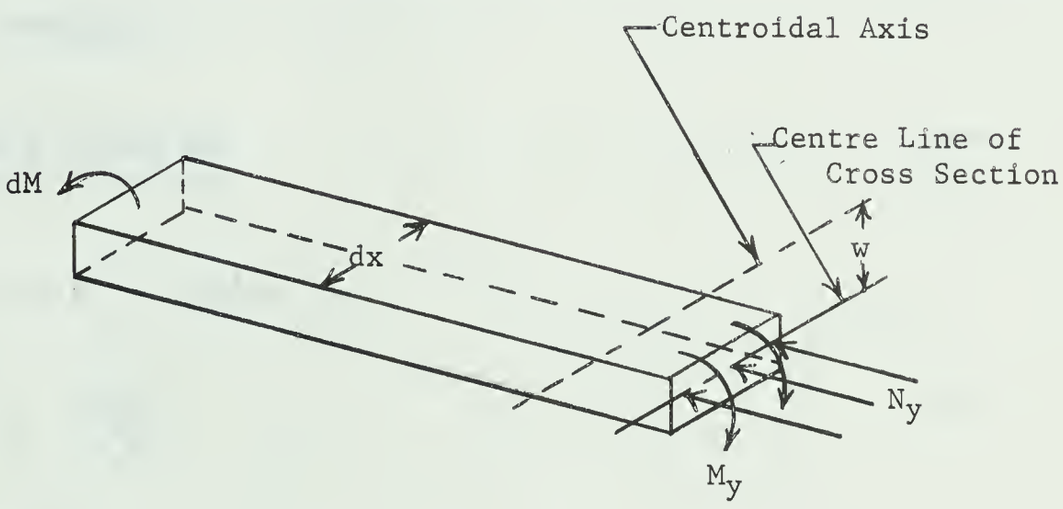

FIG. 1.7 PLATE STRIP

For ease in evaluating Eqn. 1.3-1, it is advantageous to integrate with respect to η.

Since the slope of the transverse deflection curve is small compared to unity, the curvature in the transverse direction can be written as $\frac{1}{R_x} = \frac{d^2w}{dx^2}$. Eqn. 1.2-5 shows that w_o is a linear function of x and $w = w_o + \zeta$ (Eqn. 1.2-4) thus, $1/R_x$ can be written as

$$\frac{1}{R_x} = \frac{d^2\zeta}{dx^2} . \qquad 1.3\text{-}2$$

The equation for M_y becomes

$$M_y = \frac{-Et^3}{12(1 - \mu^2)} \left[\frac{1}{R} + \mu \frac{d^2\zeta}{dx^2}\right] . \qquad 1.3\text{-}3$$

where $\frac{1}{R} \doteq \frac{1}{R_y}$.

Since ζ is a function of η, then by applying the rules of differentiation the following is obtained:

$$\frac{d^2\zeta}{dx^2} = \frac{d^2\zeta}{d\eta^2}\left[\frac{d\eta}{dx}\right]^2 + \frac{d^2\eta}{dx^2}\frac{d\zeta}{d\eta} . \qquad 1.3\text{-}4$$

Let the equation for ζ be written as

$$\zeta = \frac{1}{\eta}[F'] - w_o - \frac{6\mu b^2}{\lambda^4 R} \qquad 1.3\text{-}5$$

where F' is defined as

$$F' = A\ ber'\eta + B\ bei'\eta + C\ ker'\eta + D\ kei'\eta . \qquad 1.3\text{-}6$$

By making appropriate substitutions, Eqn. 1.3-4 becomes

$$\frac{d^2\zeta}{dx^2} = \left[\frac{2}{\eta^3}F' - \frac{2}{\eta^2}F'' + \frac{1}{\eta}F''' - \frac{t_o(1 + k)}{2\lambda^2}\right]\left(\frac{2\lambda^2}{b\eta}\right)^2$$

$$+ \left[\frac{1}{\eta^2}F' - \frac{1}{\eta}F'' + \frac{\eta t_o(1 + k)}{2\lambda^2}\right]\left(\frac{4\lambda^2}{b^2\eta^3}\right). \qquad 1.3\text{-}7$$

The double and triple prime of F are the second and third derivatives respectively of F with respect to η.

The membrane force N_y can be calculated from the membrane stress,

yielding

$$N_y = \int_{\frac{-t}{2}}^{\frac{t}{2}} \sigma_y \, dz' \qquad 1.3\text{-}8$$

where z' is measured from the center line of the cross section and t is the thickness of the plate at the point under consideration. Evaluation of Eqn. 1.3-8 yields

$$N_y = \frac{-Etw}{R_y}$$

but, since $R_y \doteq R$ then

$$N_y = \frac{-Etw}{R} \, . \qquad 1.3\text{-}9$$

From Eqns. 1.3-1, 1.3-3, 1.3-7, and 1.3-9, the following was obtained:

$$M = \frac{Eb t_o^3}{96\lambda^8(1-\mu^2)} \int_{\alpha}^{\varepsilon} \left[\frac{\eta^7}{R} + \frac{4\mu\lambda^4}{b^2}(3\eta^2 F' - 3\eta^3 F'' + \eta^4 F''') \right] d\eta$$
$$+ \frac{bEt_o}{2\lambda^4 R} \int_{\alpha}^{\varepsilon} \eta^3 \left[\frac{1}{\eta} F' - \frac{6\mu b^2}{\lambda^4 R} \right]^2 d\eta \, . \qquad 1.3\text{-}10$$

The limits of integration ε and α are obtained from the relationship

$$\eta = 2\lambda\left(1 - \frac{x}{b} + \beta\right)^{\frac{1}{2}} \, .$$

The original limits of integration were $x = b$ and $x = 0$. Due to the transformation this yields $\eta = 2\lambda\beta^{\frac{1}{2}}$ and $\eta = 2\lambda(1+\beta)^{\frac{1}{2}}$ respectively. For simplicity ε and α are defined as

$$\varepsilon = 2\lambda(\beta)^{\frac{1}{2}}$$

and $\alpha = 2\lambda(1+\beta)^{\frac{1}{2}}$.

Integration[13] of Eqn. 1.3-10 leads to the following:

$$M = \left\langle \frac{Ebt_o^3}{96\lambda^8(1-\mu^2)} \left\{ \frac{\eta^8}{8R} + \right.\right.$$

$$\frac{4\mu\lambda^4}{b^2} \left[A(\eta^4 \operatorname{ber}''\eta - 7\eta^3 \operatorname{ber}'\eta + 24\eta^2 \operatorname{ber}\eta - 48\eta \operatorname{bei}'\eta) \right.$$

$$+ B(\eta^4 \operatorname{bei}''\eta - 7\eta^3 \operatorname{bei}'\eta + 24\eta^2 \operatorname{bei}\eta + 48\eta \operatorname{ber}'\eta)$$

$$+ C(\eta^4 \operatorname{ker}''\eta - 7\eta^3 \operatorname{ker}'\eta + 24\eta^2 \operatorname{ker}\eta - 48\eta \operatorname{kei}'\eta)$$

$$\left. \left. + D(\eta^4 \operatorname{kei}''\eta - 7\eta^3 \operatorname{kei}'\eta + 24\eta^2 \operatorname{kei}\eta + 48\eta \operatorname{ker}'\eta) \right] \right\}$$

$$+ \frac{Ebt_o}{2\lambda^4 R} \left\{ \frac{A^2 + B^2}{2}\eta \, (\operatorname{ber}_1\eta \operatorname{bei}_1'\eta - \operatorname{ber}_1'\eta \operatorname{bei}_1\eta) \right.$$

$$+ \frac{A^2 - B^2}{4}\eta^2 \, (2 \operatorname{ber}_1\eta \operatorname{bei}_1\eta - \operatorname{ber}\eta \operatorname{bei}_2\eta - \operatorname{ber}_2\eta \operatorname{bei}\eta)$$

$$+ \frac{C^2 + D^2}{2}\eta \, (\operatorname{ker}_1\eta \operatorname{kei}_1'\eta - \operatorname{ker}_1'\eta \operatorname{kei}_1\eta)$$

$$+ \frac{C^2 - D^2}{4}\eta^2 \, (2 \operatorname{ker}_1\eta \operatorname{kei}_1\eta - \operatorname{ker}\eta \operatorname{kei}_2\eta - \operatorname{ker}_2\eta \operatorname{kei}\eta)$$

$$- \frac{AB}{2}\eta^2 \, (\operatorname{ber}_1^2\eta - \operatorname{ber}\eta \operatorname{ber}_2\eta - \operatorname{bei}_1^2\eta + \operatorname{bei}\eta \operatorname{bei}_2\eta)$$

$$- \frac{CD}{2}\eta^2 \, (\operatorname{ker}_1^2\eta - \operatorname{ker}\eta \operatorname{ker}_2\eta - \operatorname{kei}_1^2\eta + \operatorname{kei}\eta \operatorname{kei}_2\eta)$$

$$- \frac{AC + BD}{2}\eta \, (\operatorname{ber}_1'\eta \operatorname{kei}_1\eta - \operatorname{ber}_1\eta \operatorname{kei}_1'\eta - \operatorname{bei}_1'\eta \operatorname{ker}_1\eta + \operatorname{bei}_1\eta \operatorname{ker}_1'\eta)$$

$$- \frac{AD - BC}{2}\eta \, (\operatorname{ker}_1'\eta \operatorname{ber}_1\eta - \operatorname{ker}_1\eta \operatorname{ber}_1'\eta + \operatorname{kei}_1'\eta \operatorname{bei}_1\eta - \operatorname{kei}_1\eta \operatorname{bei}_1'\eta)$$

$$+ \frac{AC - BD}{4}\eta^2 \, (2 \operatorname{ber}_1\eta \operatorname{kei}_1\eta - \operatorname{ber}\eta \operatorname{kei}_2\eta - \operatorname{ber}_2\eta \operatorname{kei}\eta$$
$$+ 2 \operatorname{bei}_1\eta \operatorname{ker}_1\eta - \operatorname{bei}\eta \operatorname{ker}_2\eta - \operatorname{bei}_2\eta \operatorname{ker}\eta)$$

$$+ \frac{AD + BC}{4}\eta^2 \, (2 \operatorname{bei}_1\eta \operatorname{kei}_1\eta - \operatorname{bei}\eta \operatorname{kei}_2\eta - \operatorname{bei}_2\eta \operatorname{kei}\eta$$
$$- 2 \operatorname{ber}_1\eta \operatorname{ker}_1\eta + \operatorname{ber}\eta \operatorname{ker}_2\eta + \operatorname{ber}_2\eta \operatorname{ker}\eta)$$

$$- \frac{12\mu b^2}{\lambda^4 R} \left[A(\eta^2 \operatorname{ber}\eta - 2\eta \operatorname{bei}'\eta) + B(\eta^2 \operatorname{bei}\eta + 2\eta \operatorname{ber}'\eta) \right.$$
$$\left. + C(\eta^2 \operatorname{ker}\eta - 2\eta \operatorname{kei}'\eta) + D(\eta^2 \operatorname{kei}\eta + 2\eta \operatorname{ker}'\eta) \right]$$

$$\left. \left. + \frac{9\mu^2 b^4 \eta^4}{\lambda^8 R^2} \right\} \right\rangle_{\eta=\alpha}^{\eta=\varepsilon} \qquad 1.3\text{-}11$$

where the subscripts on the preceeding Bessel functions indicate the order of the function. No subscript indicates a Bessel function of order zero. The solution to Eqn. 1.3-11 was obtained using an IBM 7040/1401 digital computer. Details of this solution along with the solution for the constants of integration appear in Appendix A.

1.4 DISCUSSION OF THEORETICAL RESULTS

Theoretical curves for the moment-curvature relationship were obtained for different parameter variations. The effect on the moment-curvature relationship when k was increased while other parameters were held constant is shown in Fig. 1.8 when the plate was turned upside down (concave side down). As k was increased, the slope of the curves increased sharply due to the increased plate stiffness, however, a maximum moment was reached after which the moment decreased for an increase in curvature. The point of instability was reached when the effect of the membrane and transverse bending forces were large enough to flatten out the cross section of the plate. As the camber decreased due to the increased loads, the plate began to act as a flat plate. Theoretically, for large curvatures, the moment-curvature relationships for different k values should approach the case where $k = 0$. This is shown to be the result in Fig. 1.8.

In Fig. 1.9, moment-curvature relationships were plotted for the case when the plate was bent with the concave side up. In the cross section used in Fig. 1.8, the membrane forces and the transverse bending action are both acting to distort the section anticlastically. When the plate had the concave side up (Fig. 1.9), the

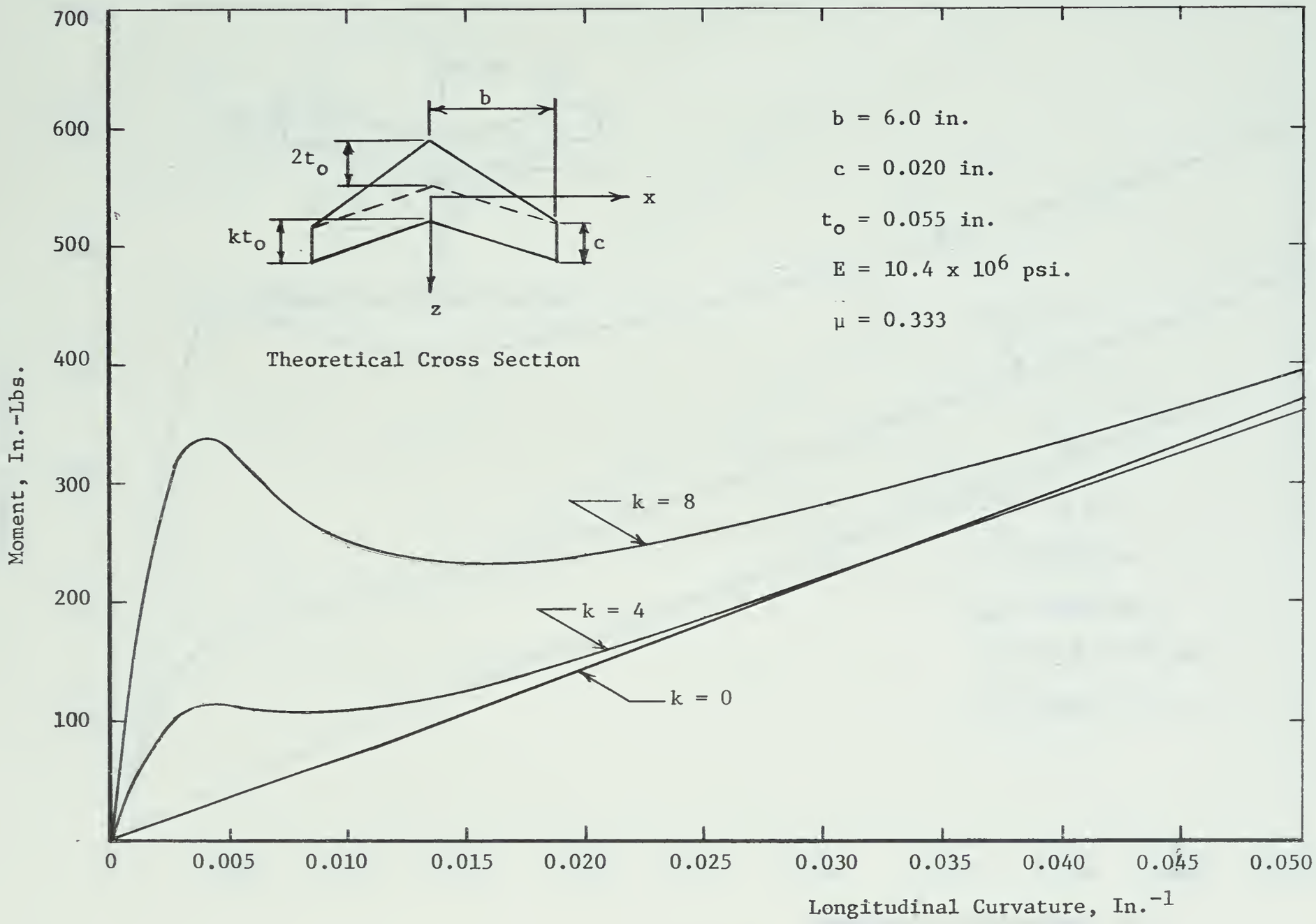

FIG. 1.8 THEORETICAL MOMENT-CURVATURE RELATIONSHIPS FOR VARIATION IN k
(CONCAVE SIDE DOWN)

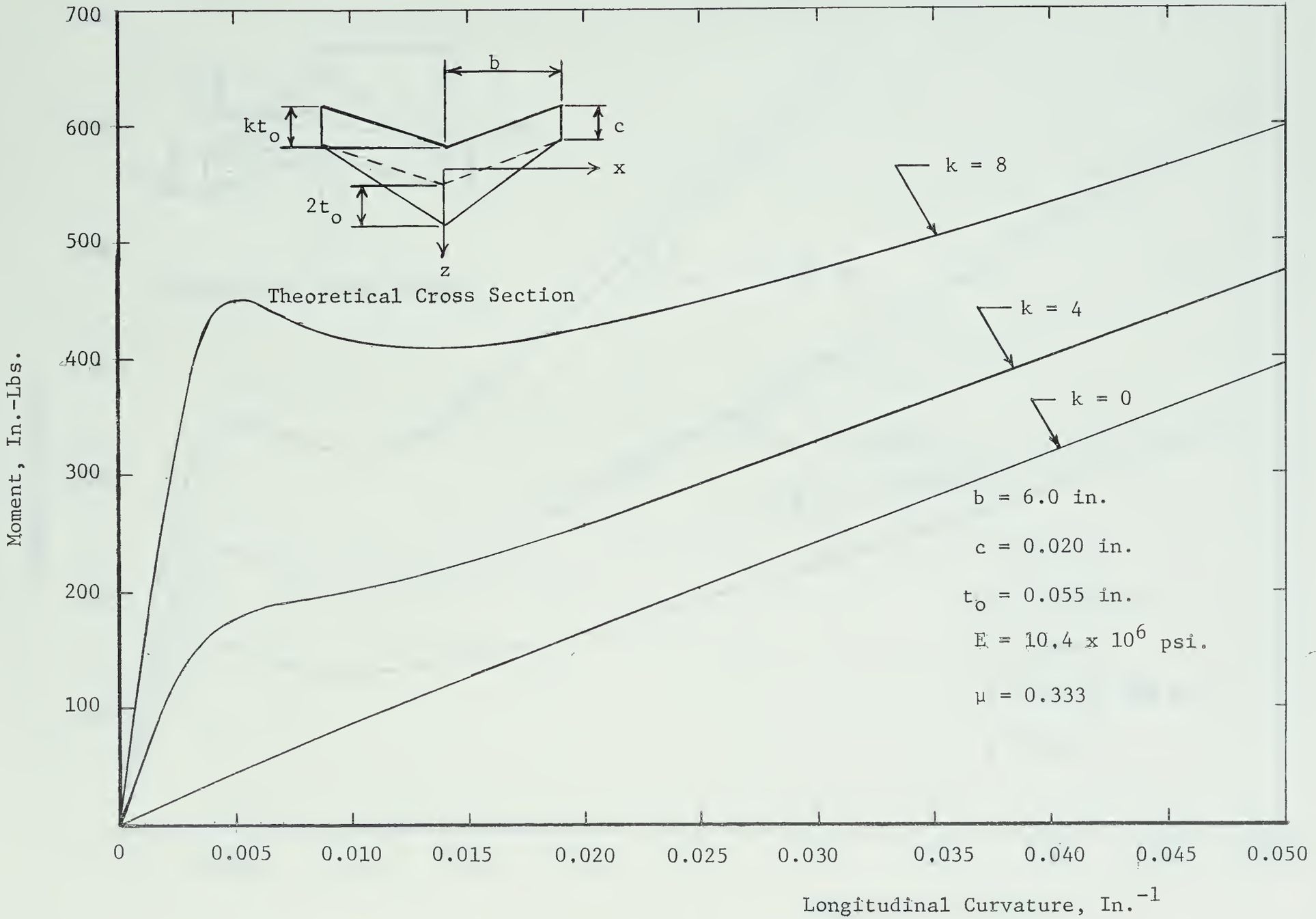

FIG. 1.9 THEORETICAL MOMENT-CURVATURE RELATIONSHIPS FOR VARIATION IN k
(CONCAVE SIDE UP)

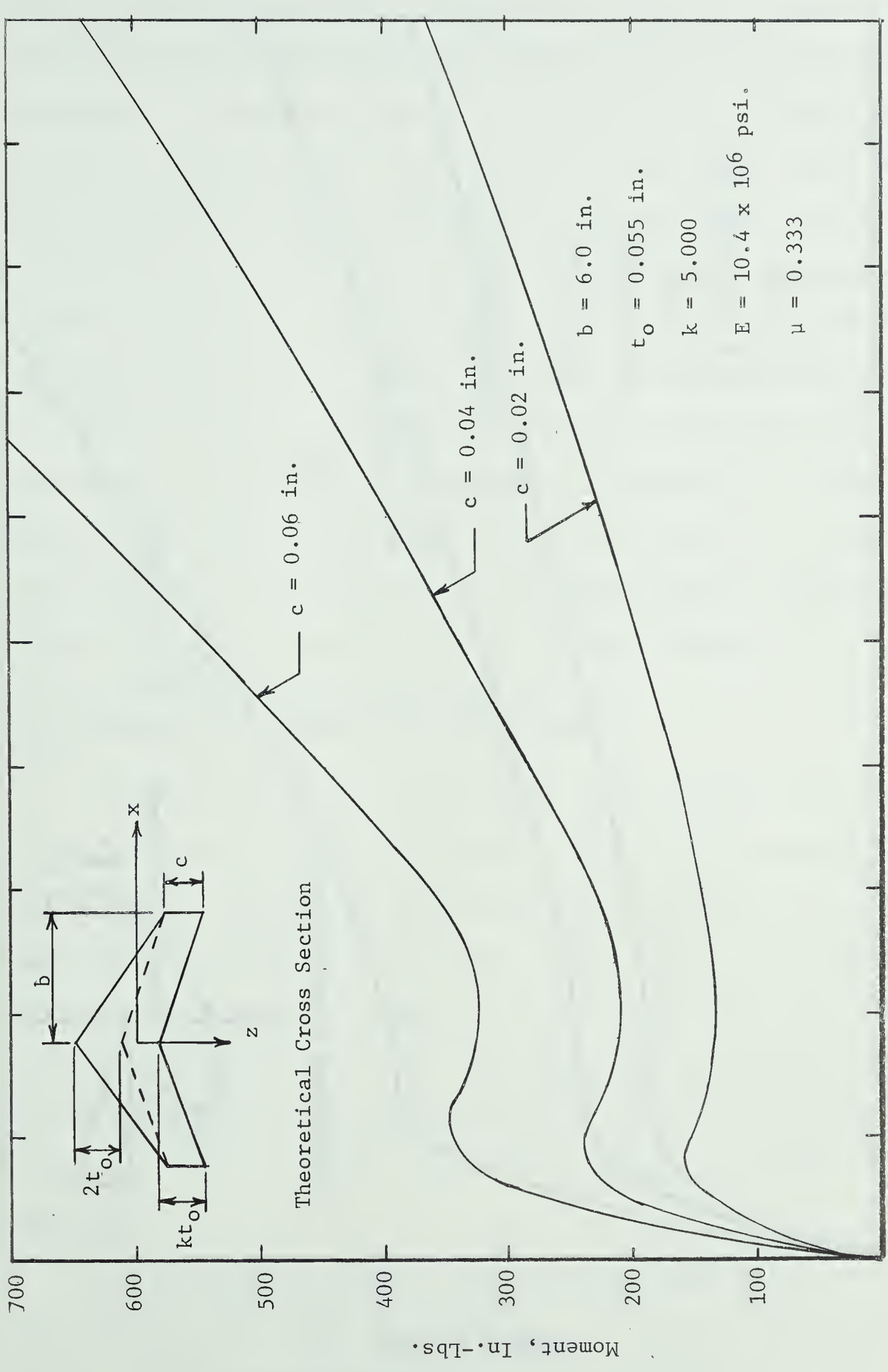

FIG. 1.10 THEORETICAL MOMENT-CURVATURE RELATIONSHIPS FOR VARIATION IN c
(CONCAVE SIDE DOWN)

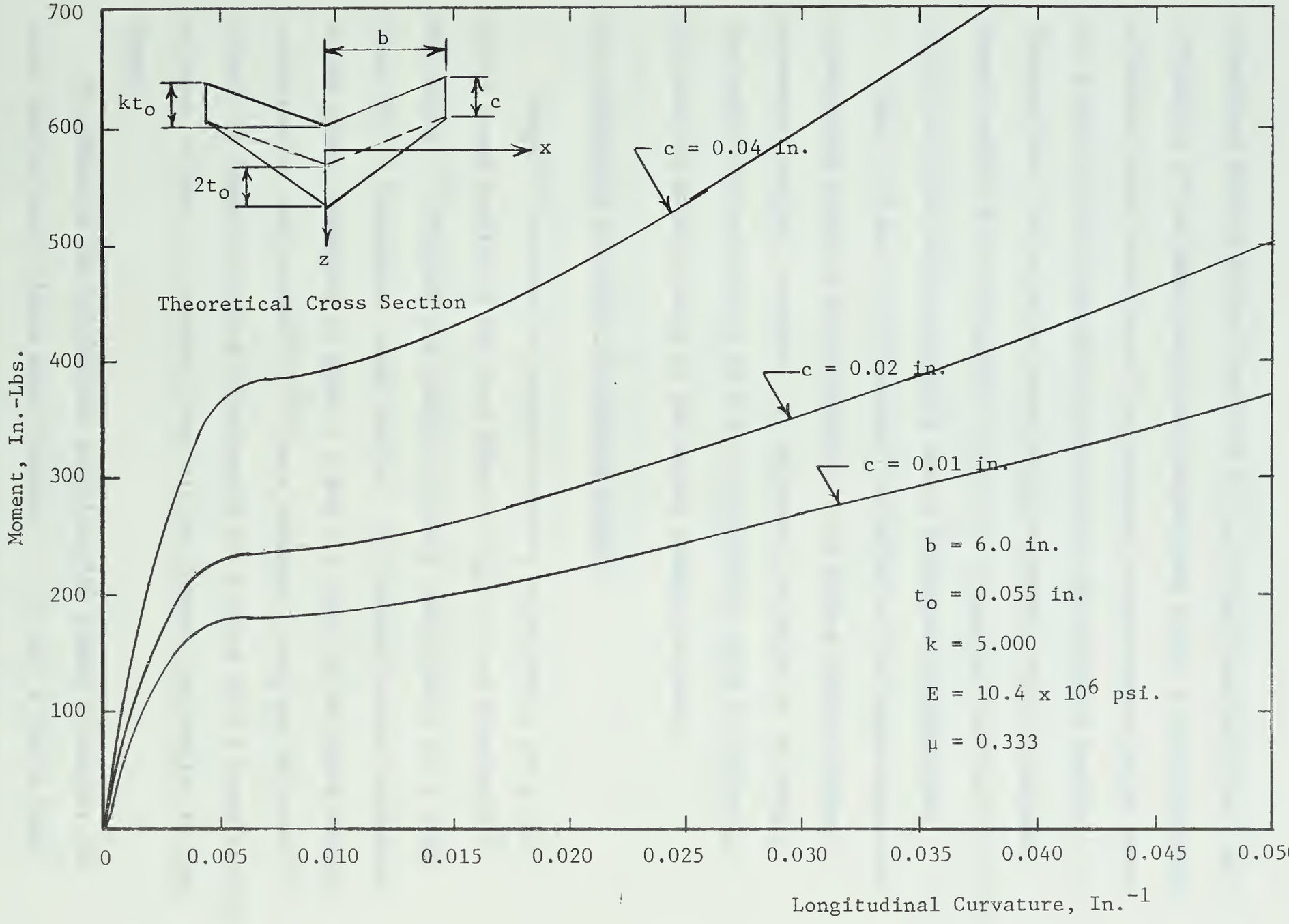

FIG. 1.11 THEORETICAL MOMENT-CURVATURE RELATIONSHIPS FOR VARIATION IN c
(CONCAVE SIDE UP)

transverse bending action distorted the plate anticlastically but the components of the membrane forces counteracted this. A critical point is reached when the effect of the membrane forces becomes larger than the effect of the transverse bending action and the cross section flattens out. It is due to these opposite effects that the maximum moment reached for this section (Fig. 1.9) is greater than for Fig. 1.8 before the cross section distorts into a flattened configuration.

Figs. 1.10 and 1.11 illustrate the effect on the moment-curvature relationship when the edge thickness, c, is varied while the other parameters are held constant. As expected, the value of the moment increases with an increase in c for a particular value of curvature, although the general shape of the curves remains the same.

1.5 COMPARISON OF THEORY TO PREVIOUS RESULTS

Flügge[3] obtained the moment-curvature relationship for a plate with a cross section of the type shown in Fig. 1.1 and Timoshenko[2] and Searle[14] obtained the moment-curvature relationship for a flat plate with a rectangular cross section. By changing certain parameters in the theory developed in Secs. 1.2 and 1.3, both of the cross sections considered by the authors[2,3,14] were obtained. Fung and Wittrick[6] stated the moment-curvature relationship for a plate with a cross section as shown in Fig. 1.2, however, they did not present any results in their paper.

In comparing the theoretical solution with Flügge's results, the cross section had a finite edge thickness, $c > 0$, and a finite taper $t_o > 0$. The cross section and the results are shown in Fig. 1.12.

The theoretical solution was obtained by setting $k = 0$. Flügge's results and linear theory shown are only approximate as they were obtained from a graph.

In comparing the developed theory with the theory for a plate with a rectangular cross section, t_o and k have to be set equal to zero. As t_o approaches zero, λ approaches infinity and no solution can be obtained. For comparison, t_o was decreased to about 10 percent of the edge thickness. The cross section considered and the comparison is shown in Fig. 1.13. It is evident that if t_o approached zero the two theories would yield the same results.

Figs. 1.12 and 1.13 indicate that agreement between different solutions is good. In the following sections, experimental verification is presented for plates with different variations of the cross section as shown in Fig. 1.5.

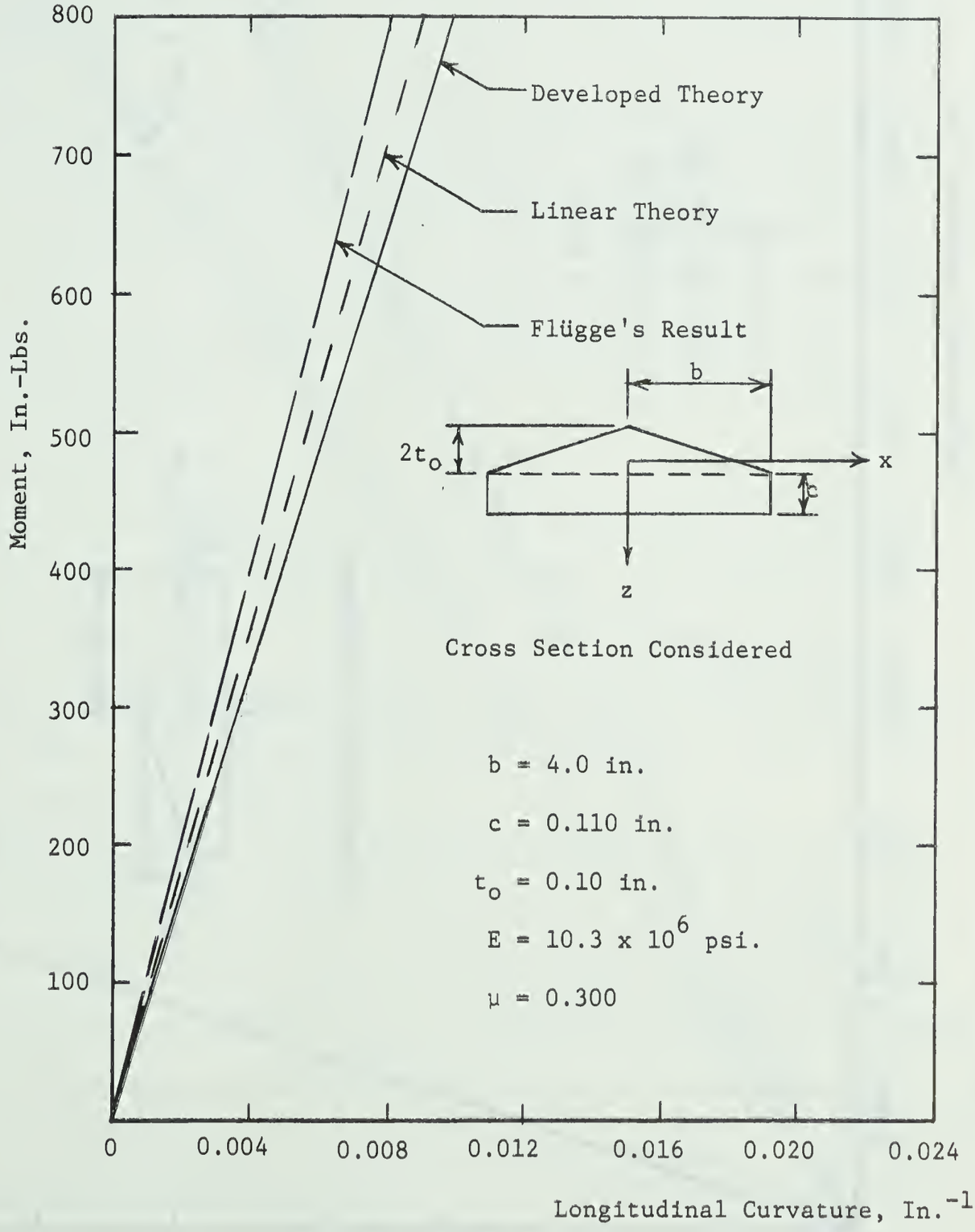

FIG. 1.12

COMPARISON OF THEORY WITH PREVIOUS WORK FOR BITRAPEZOIDAL CROSS SECTION

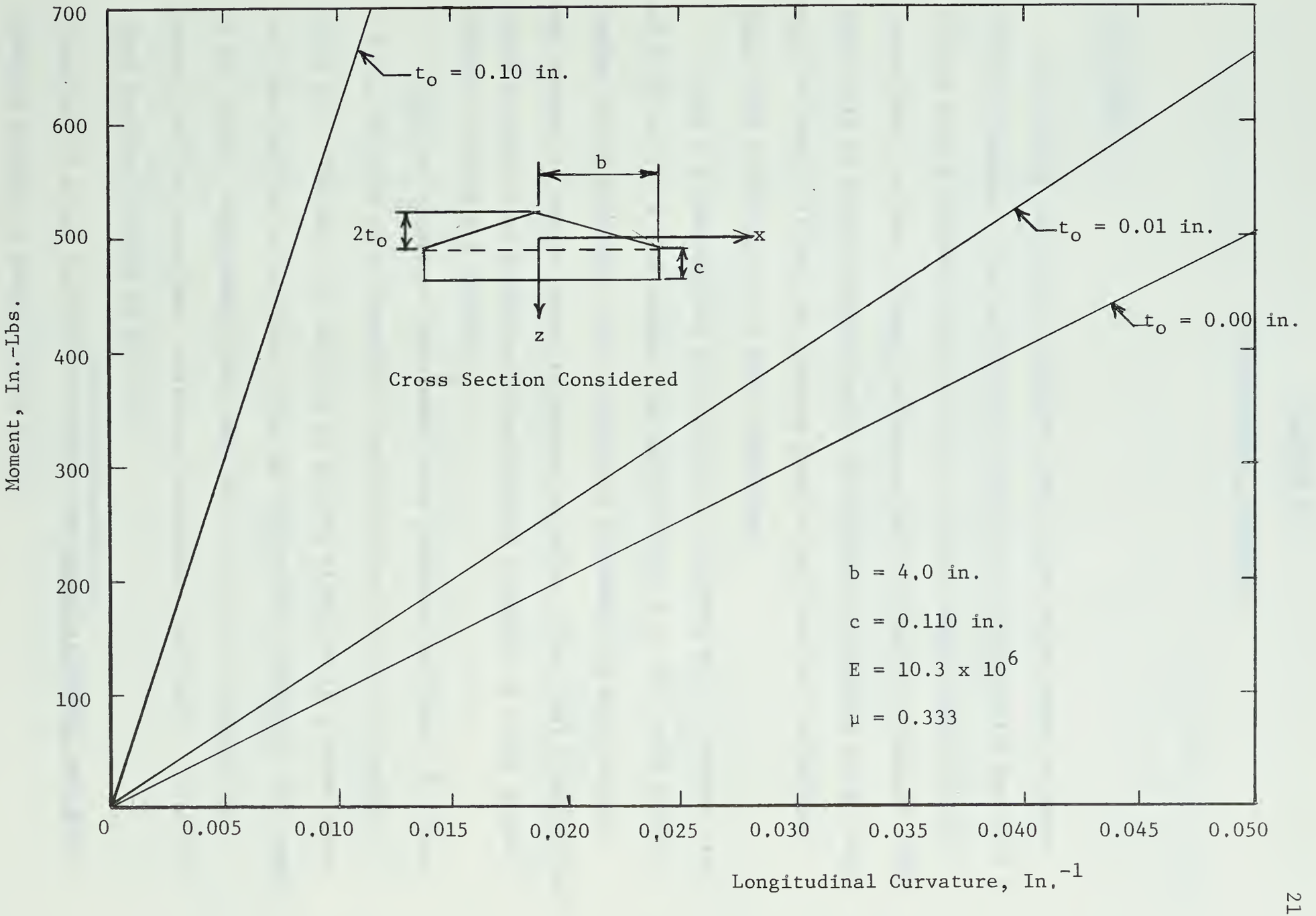

FIG. 1.13 COMPARISON WITH LINEAR THEORY FOR A RECTANGULAR CROSS SECTION PLATE

CHAPTER II

EXPERIMENTAL APPARATUS

2.1 PLATES

The plates tested were machined from a flat rolled sheet of Alcoa 7075-T6* Aluminum. The modulus of elasticity of this material was 10.4 x 10^6 psi with a Poisson's ratio of 0.333. With a lower modulus of elasticity than for steel, higher curvatures were obtained with smaller loads than would be possible using steel. The density of aluminum being lower than for steel, allowed an aluminum plate to act more as a weightless plate than a steel plate of equal dimensions.

Plate I-A was machined from a sheet of aluminum with a nominal size of 0.125 x 12.0 x 67.0 inches. As shown in Fig. 2.1, the cross section warped during machining. For calculation purposes, the cross section was assumed to have a linear thickness variation. The final cross section could be bent to an approximate longitudinal curvature of 0.100 inches^{-1} without yielding the material.

After the necessary experiments were performed on Plate I-A, Plate I-B was obtained by performing a "controlled bend" along the length of Plate I-A. The bend was obtained by placing Plate I-A in a press brake and then applying a line load along the centre line throughout the length of the plate. Measurements were made after every load increment to ensure that the plate bent uniformly throughout its length. The final cross section is shown in Fig. 2.2.

---

*Properties of alloy used were obtained from Alcoa Structural Hand Book Aluminum Company of America 1956, p. 35.

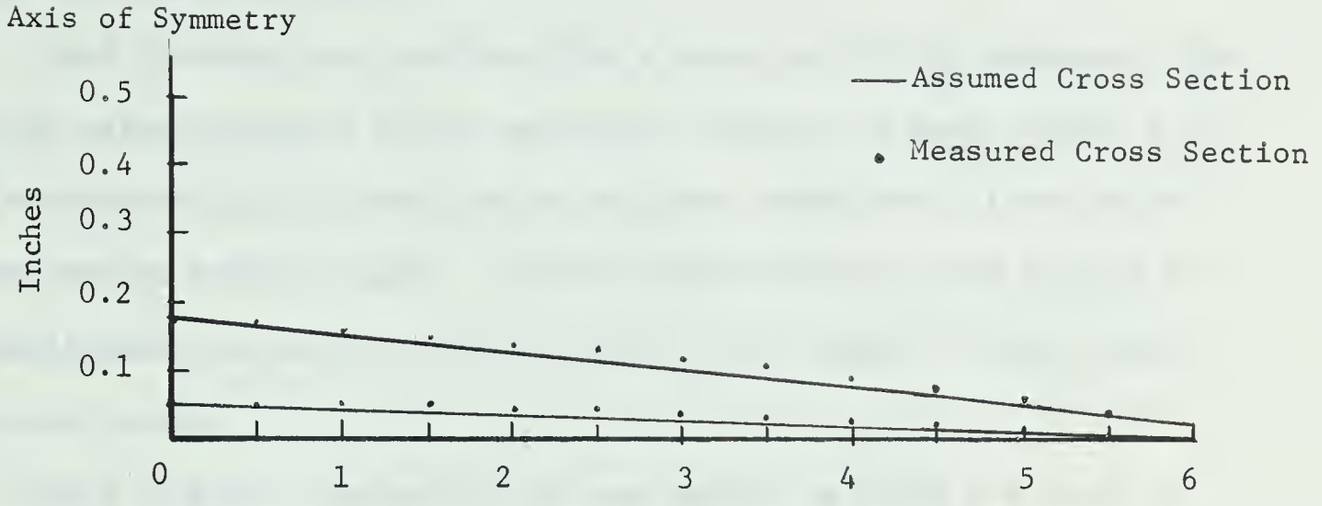

FIG. 2.1 CROSS SECTION OF PLATE I-A

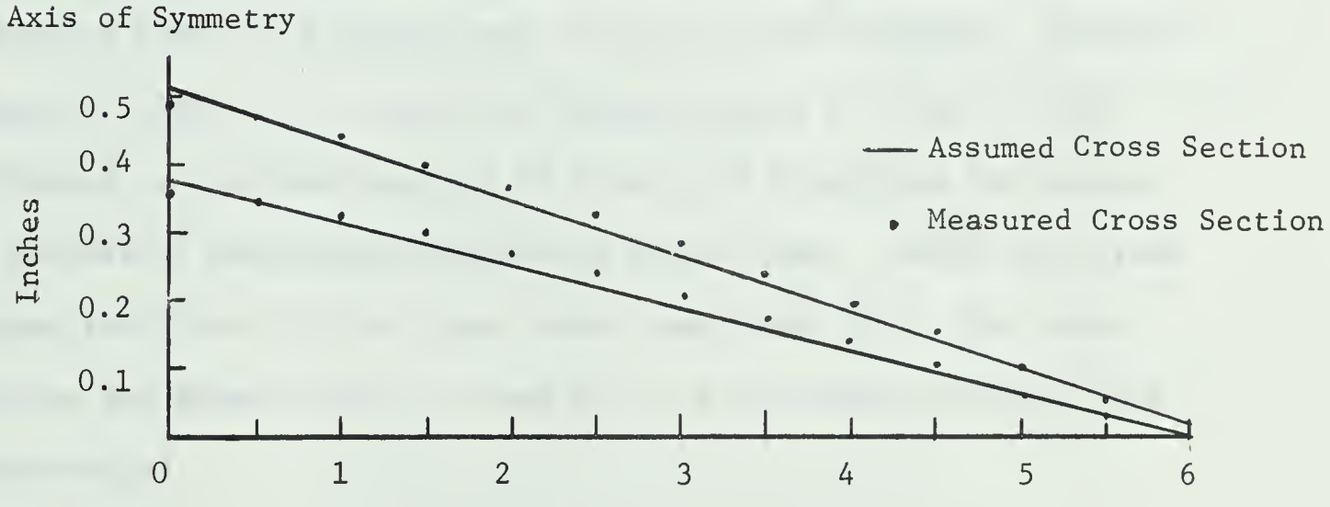

FIG. 2.2 CROSS SECTION OF PLATE I-B

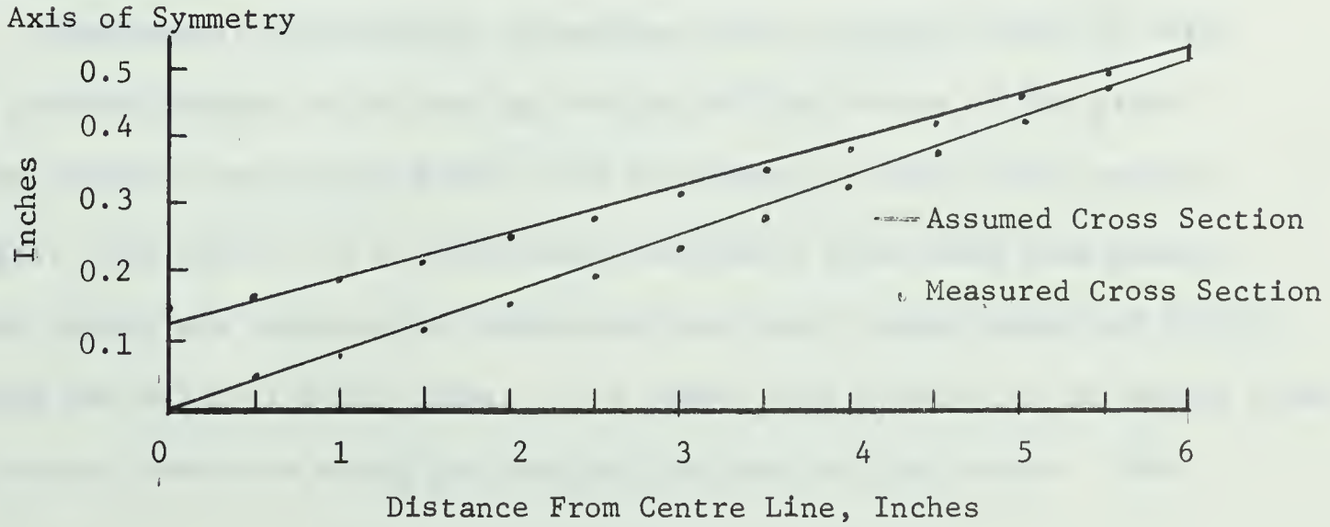

FIG. 2.3 CROSS SECTION OF PLATE I-C

Plate I-C was obtained by turning Plate I-B upside down. The cross section is shown in Fig. 2.3.

Plate II-A was also machined from a sheet of 7075-T6 aluminum. The section warped slightly during machining; however, as seen in Fig. 2.4, the warping was quite linear and an accurate description of the actual cross section could be made. The final cross section could be bent to a longitudinal curvature of approximately 0.054 inches^{-1} before yeilding would occur.

Plate II-B was obtained in the same manner as Plate I-B (i.e. by performing a"controlled bend" along the length of the plate). By turning Plate II-B upside down, Plate II-C was obtained. The difference in some of the dimensions between Plates II-B and II-C are attributed to the cross section of Plate II-B flattening out during the process of performing experiments on the Plate. Hence, the cross section for Plate II-C had less camber than Plate II-B. The cross sections are shown in Fig. 2.5 and Fig. 2.6 for Plates II-B and II-C respectively.

2.2 STRAIN GAUGES

Experimental longitudinal curvatures were calculated from the bending strains induced in the top and bottom surface fibres of the plate. These strains were measured with Budd Instruments type C12-121 strain gauges. The C12-121 is an electrical resistance metal film type gauge. These gauges are temperature compensated and have a gauge length of 0.122 inches and width of 0.125 inches. The gauges were mounted on the centre line at various positions along the longitudinal axes of the plates. (See

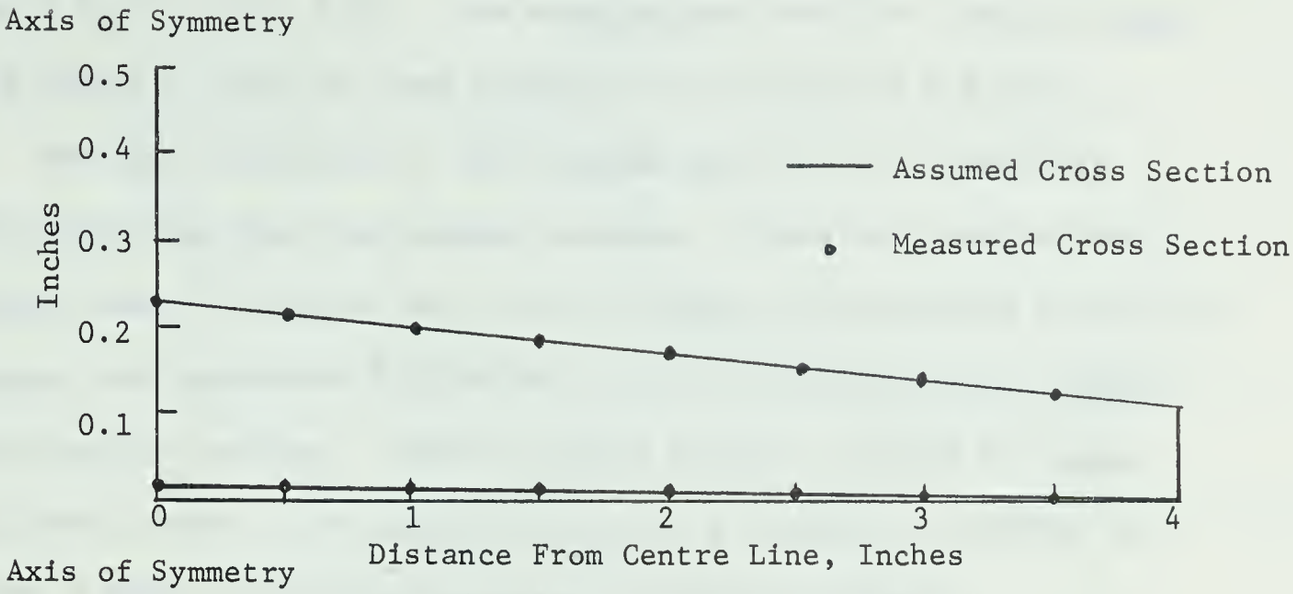

FIG. 2.4 CROSS SECTION OF PLATE II-A

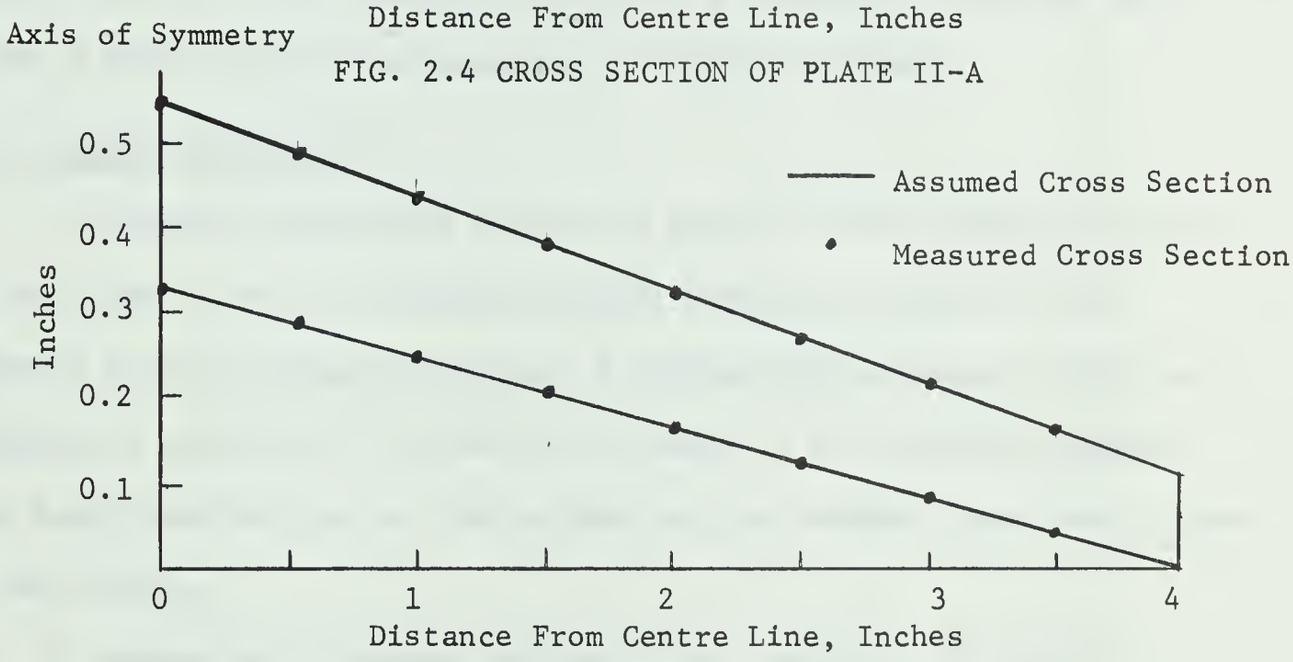

FIG. 2.5 CROSS SECTION OF PLATE II-B

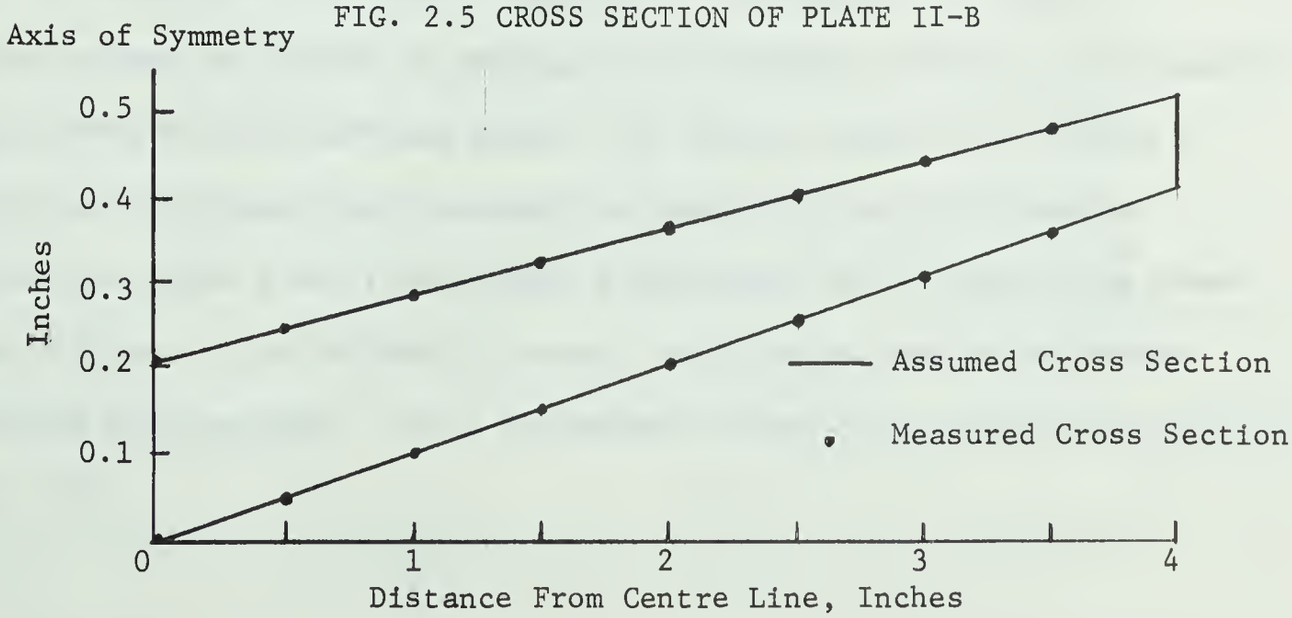

FIG. 2.6 CROSS SECTION OF PLATE II-C

Fig. 2.7, 2.8, 2.9, 2.10). The mounting was such that the top gauges were directly above the ones mounted on the bottom of the plate.

Two main advantages of these gauges were the low transverse sensitivity and the thin backing material. Since the longitudinal strains were of interest only, then by using low transverse sensitivity gauges, the transverse strains had very little effect on the longitudinal strain readings. Thinner backing material allowed the gauge to be placed closer to the surface for which a reading is desired, and hence, a more accurate surface strain could be obtained.

2.3 LOADING APPARATUS

A uniformly distributed moment was applied to the transverse ends of the plate by means of bolting the two ends of the plate to two separate one-inch diameter shafts. A fifteen-inch diameter pulley was fastened to each end of the shaft. By means of wire cables, hangers were hung from the rims of the pulleys and the desired loads were placed on the hangers.

To reduce the frictional effects at the supports, the shaft-pulley system was placed on bearings. The bearings rested on two channels whose surfaces were machined smooth. To further reduce the effects of friction, after each load increment was applied, the shaft-bearing system was given a small horizontal displacement on the supporting channels and then it was allowed to come to equilibrium before any strain readings were recorded. For a photographic view of the apparatus, see Fig. 2.11.

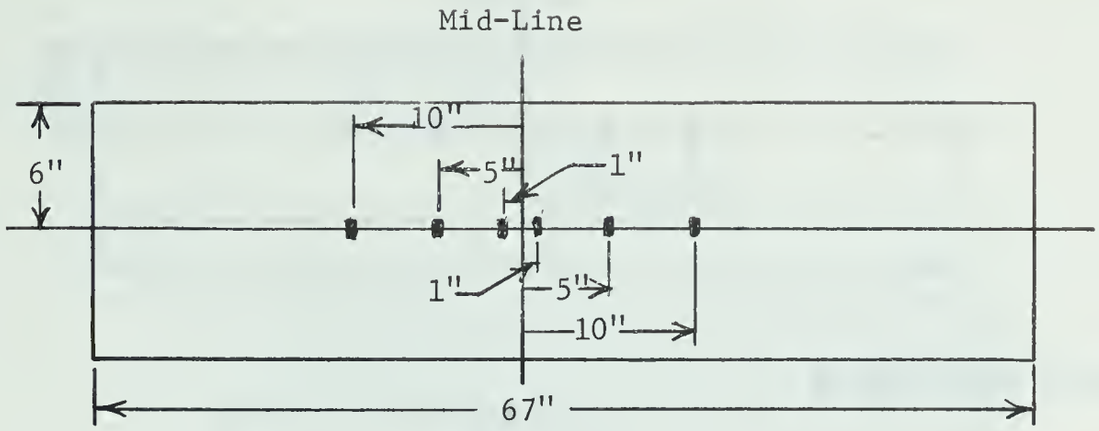

▮ Measuring Station

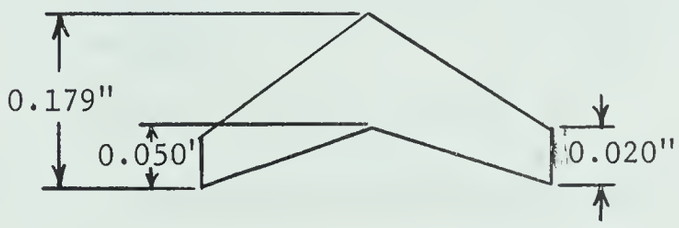

Cross Section of Plate I-A

FIG. 2.7 MEASURING STATION FOR PLATE I-A

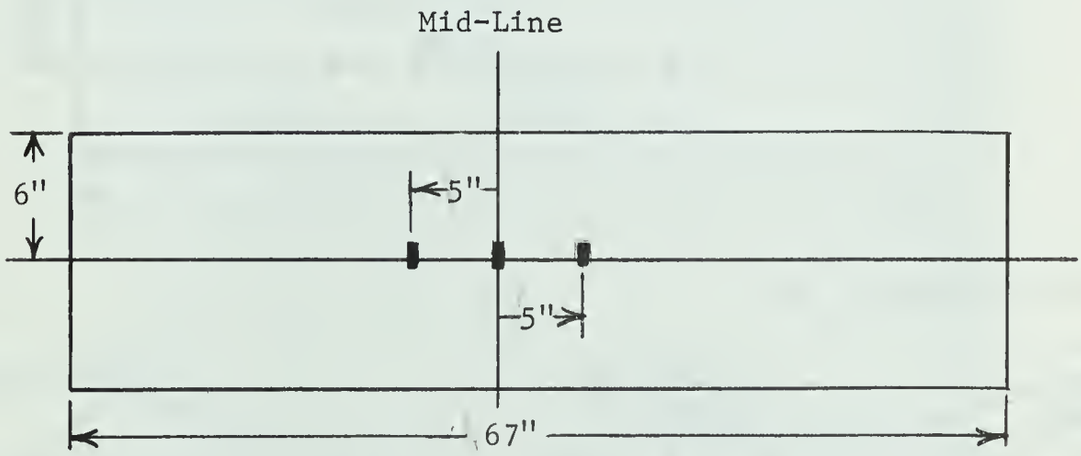

▮ Measuring Station

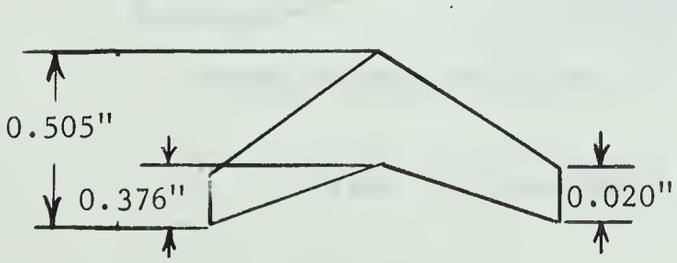

Cross Section of Plate I-B

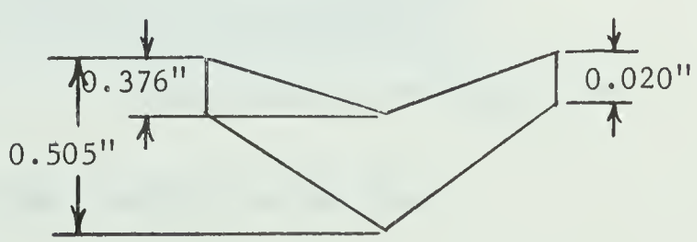

Cross Section of Plate I-C

FIG. 2.8 MEASURING STATIONS FOR PLATES I-B AND I-C

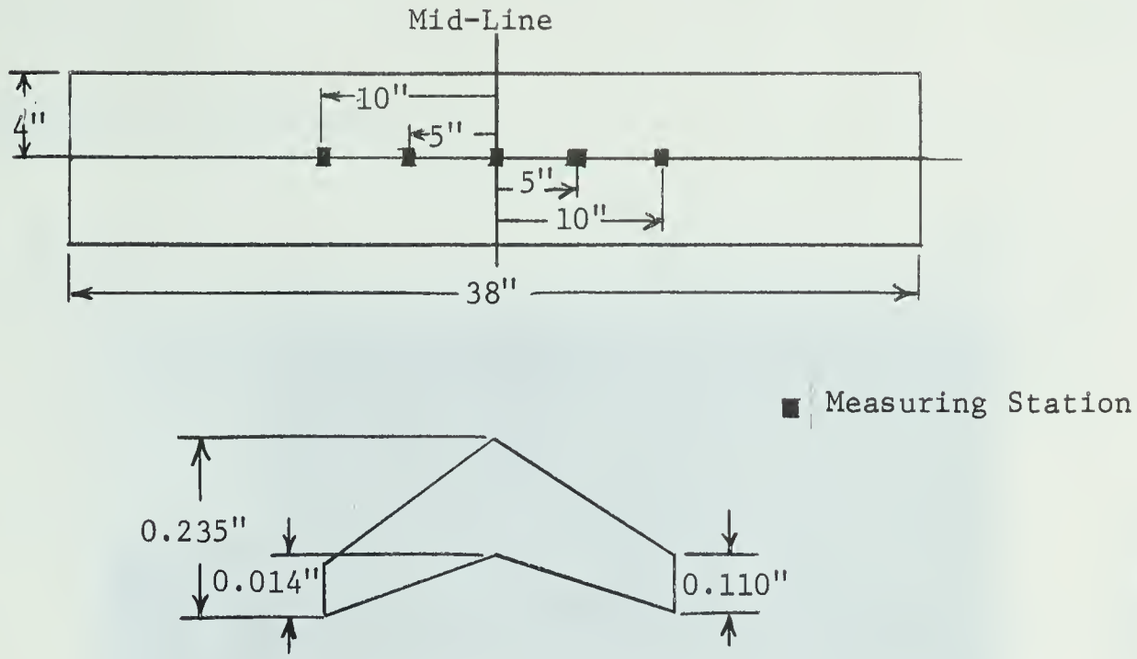

FIG. 2.9 MEASURING STATIONS FOR PLATE II-A

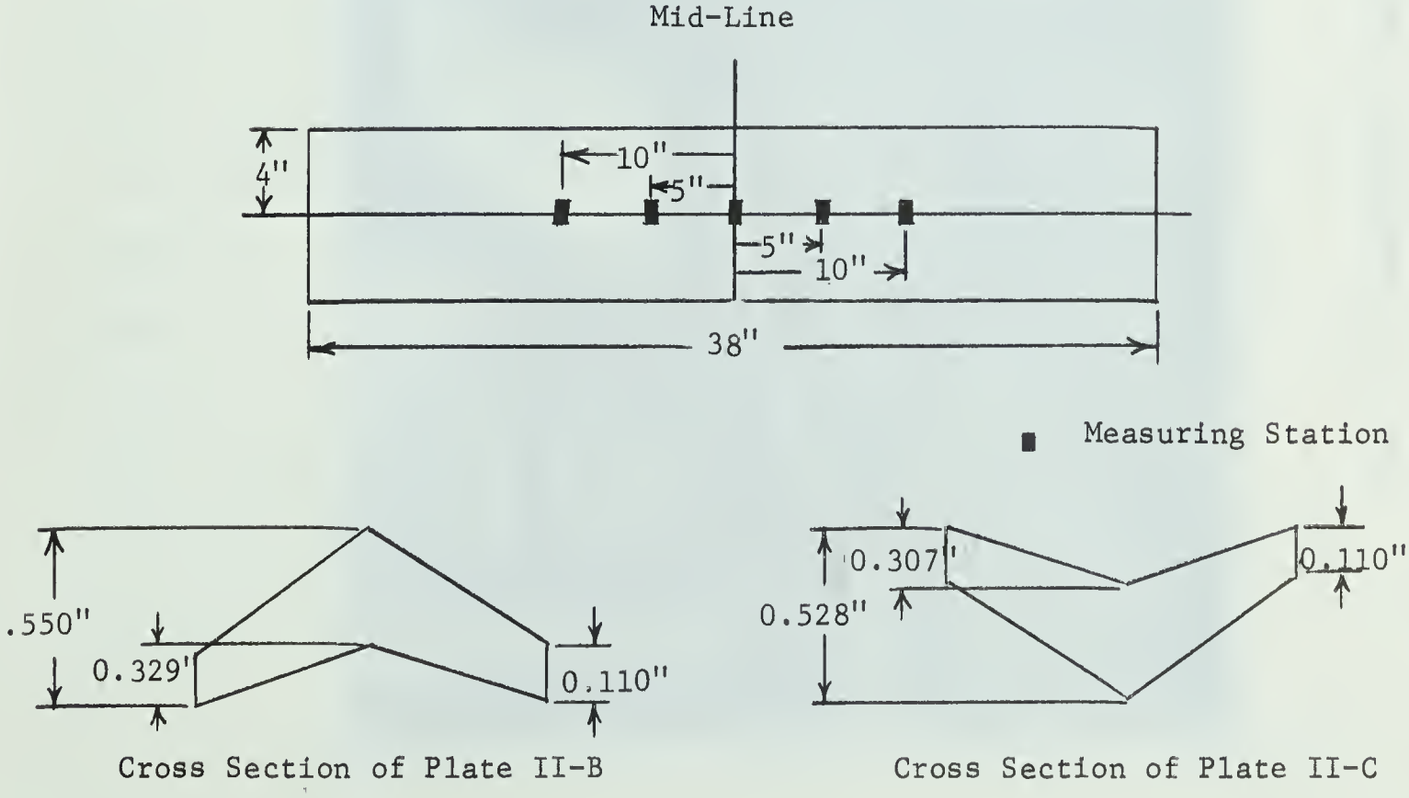

FIG. 2.10 MEASURING STATIONS FOR PLATES II-B AND II-C

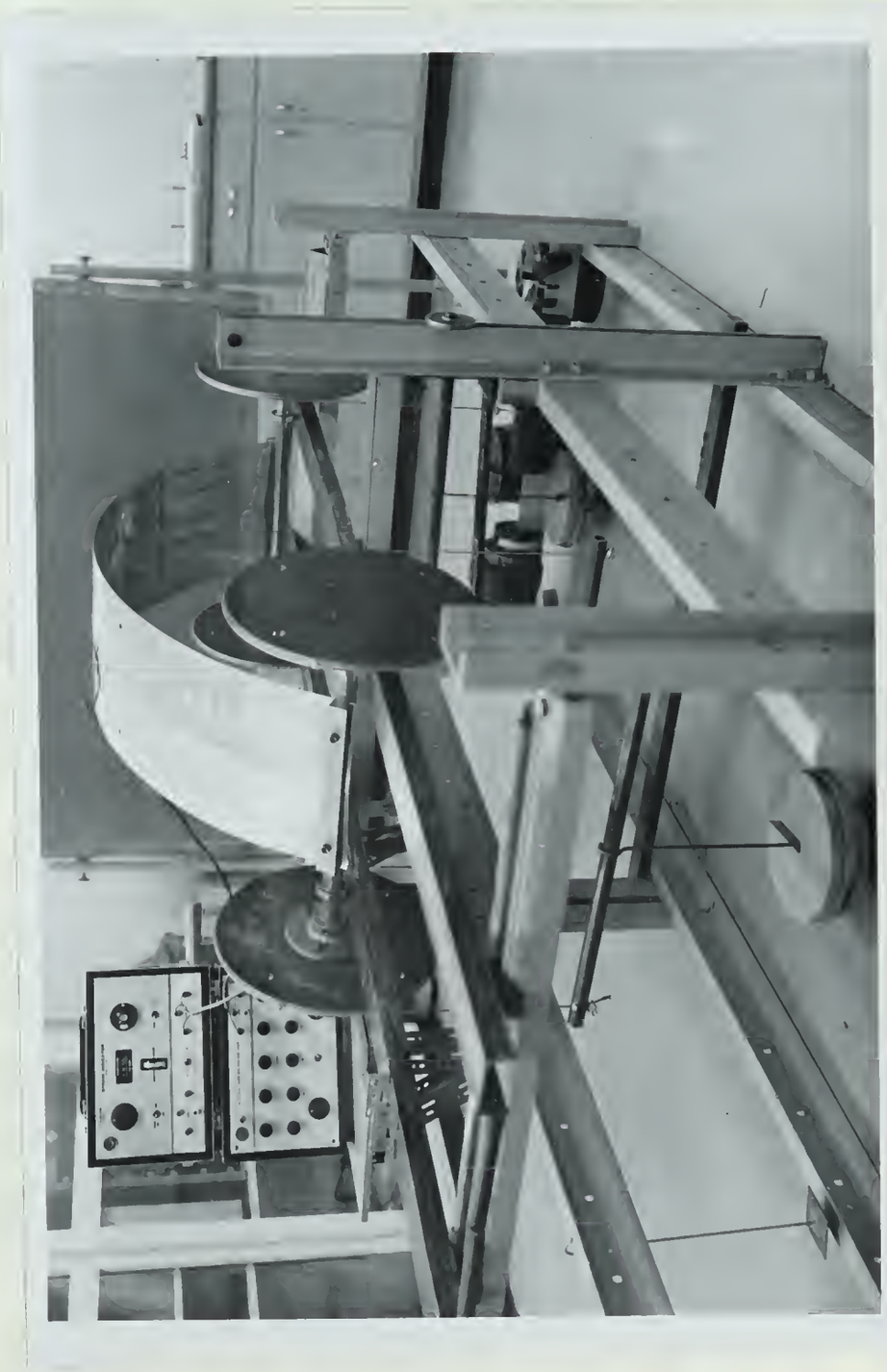

FIG. 2.11 PHOTOGRAPHIC VIEW OF LOADING APPARATUS

2.4 MEASUREMENT OF CURVATURE

The longitudinal curvatures were calculated from the strains induced in the top and bottom fibres of the plate. A BLH switching and balancing unit was used to switch from one measuring station to the next and a BLH strain indicator was used to read the strains.

For a plate in pure bending, it can be shown that

$$\frac{1}{R} = \frac{-2(e_i)_B}{t_i} \qquad 2.4\text{-}1$$

where $(e_i)_B$ = bending strain at x_i

and t_i = thickness of the plate at x_i.

However, when a plate is bent into a longitudinal curvature such that axial strains are developed in addition to bending strains, it becomes necessary to eliminate the axial strains before the curvatures can be calculated. The axial strains were eliminated by having the gauges wired in series such that the strains at the top of the plate and the strains directly at the bottom of the plate were additive giving a double output of the actual strain on the top or bottom surface. Defining the double output of the bending strain as e_B and substituting this value for $2(e_i)_B$ in Eqn. 2.4-1 the curvature becomes

$$\frac{1}{R} = \frac{-e_B}{t_i} \qquad 2.4\text{-}2$$

Using Egn. 2.4-2, a computer program was written to evaluate curvatures from the strain gauge readings (see Appendix B). Knowing both the moment and the corresponding curvature, the experimental curves were plotted.

2.5 TESTING PROCEDURE

The testing procedure used for all six plates was essentially the same. Initially, a flat support was inserted under the plate. With the flat support in place, the strain gauges were zeroed. Then the flat support was removed, allowing the plate to sag due to its own weight. Loads were then applied in desired increments. The applied load and the strain readings were recorded for each measuring station. After the maximum load had been applied, all the load was removed and the flat support was reinserted under the plate so that the zero readings could be checked.

CHAPTER III

EXPERIMENTAL AND THEORETICAL RESULTS

3.1 REMARKS ON EXPERIMENTAL RESULTS

Three different sets of strain gauge readings were obtained for each measuring station. The variation in strain for any given curvature was small, it was decided that an average obtained from three sets of readings was sufficient to establish the experimental curve. Each experimental plate was symmetrical about its longitudinal axis and the measuring stations were placed along this axis. Since the minimum number of stations on any plate was three and the maximum was six, this gave a minimum number of nine and a maximum of eighteen different readings being averaged for each point plotted.

3.2 COMPARISON BETWEEN EXPERIMENTAL AND THEORETICAL RESULTS

In the development of the theory, it was assumed that the plate was weightless; hence, when the experimental and theoretical moments were compared for a particular longitudinal curvature, it was necessary to subtract from the applied moment the moment due to the weight of the plate. It can be seen from Fig. 3.1 that the weight per unit horizontal distance varies with the distance from the mid-line at a particular longitudinal curvature. This variation must be accounted for in the correction moment. By summing moments about a section p units from the mid-line, the correction moment due to the weight of the plate can be shown to be

$$M_1 = qL(a - p) + qR\left[\sqrt{R^2 - a^2} - \sqrt{R^2 - p^2} + p\left(\arcsin\frac{a}{R} - \arcsin\frac{p}{R}\right)\right] \qquad 3.2\text{-}1$$

where M_1 = correction moment,

q = weight per unit length of plate,

p = horizontal distance from mid-line to section where correction moment is desired,

R = longitudinal radius of curvature (average R),

L = one-half the total length of plate, and

a = one-half the distance between supports.

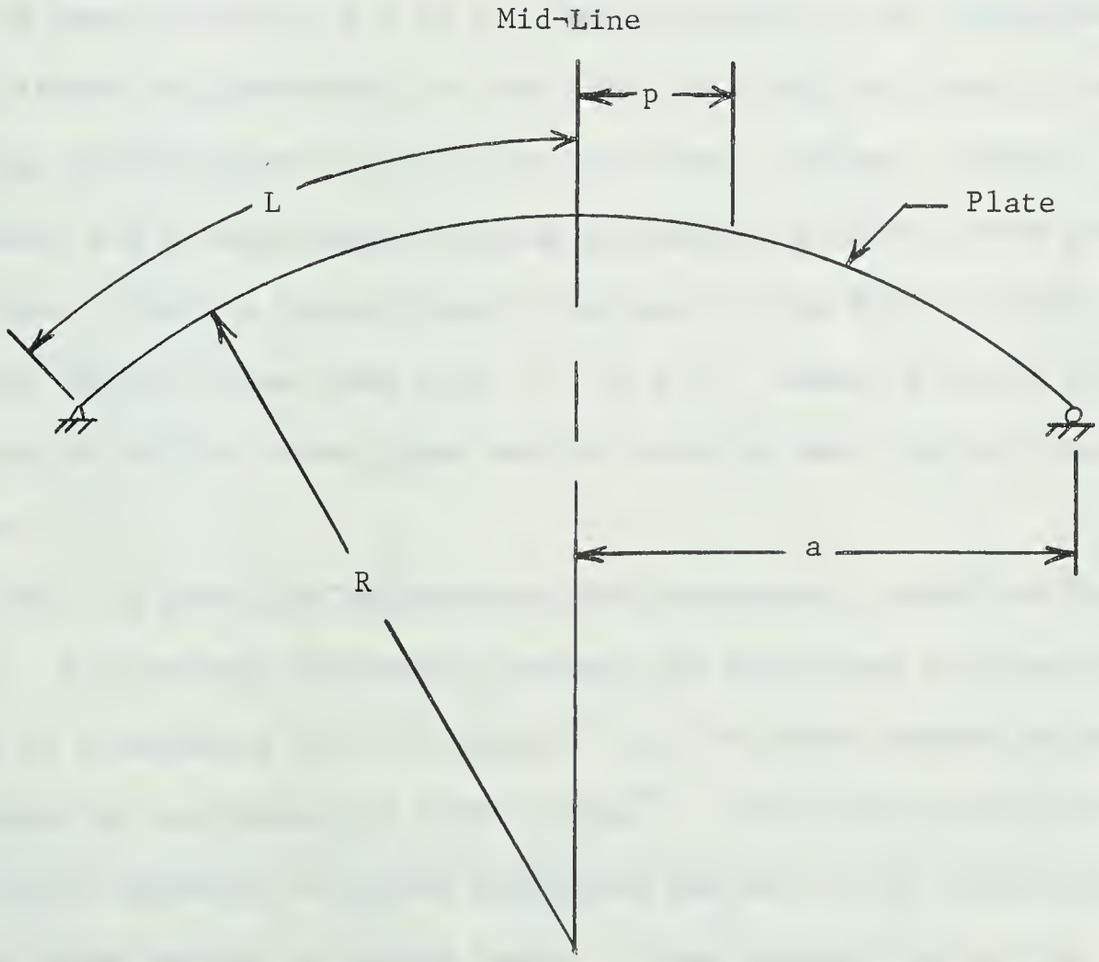

FIG. 3.1 DIAGRAM FOR OBTAINING CORRECTION MOMENT

The experimental curves were plotted and compared with theory in Figs. 3.2 to 3.7.

In measuring k for the different plates, it was found that this value varied by about 10 percent between different points on the same plate. In calculating the theoretical curves, an average value for k was used. It was found that a small change in k, for $k < 1$, produced a negligible change in the theoretical curves but a small change in k, for $k > 5$, produced large changes in the curves. Not being able to measure k accurately for the plates with $k > 5$ was a possible source of error.

3.3 DISCUSSION OF RESULTS

As seen from Figs. 3.2 to 3.7, better agreement was reached between theory and experiment for the tests involving the Plate II series than was obtained from the tests for the Plate I series. Better agreement was reached because during the machining of the cross section, the Plate II series warped linearly whereas for the Plate I series, the warping was non linear (see Figs. 2.1 to 2.6). Hence, a better approximation to the actual cross section could be made for the Plate II series.

Fig. 3.2 shows the experimental and theoretical curves for Plate I - A. A 24 percent discrepancy between the two curves is shown to occur at a curvature of 0.015 inches^{-1}, but the error reduced to only 2 percent at a curvature of 0.046 inches^{-1}. One possible reason for the better agreement at higher curvatures was due to the distortion of the cross section at higher loads. It was assumed that as the

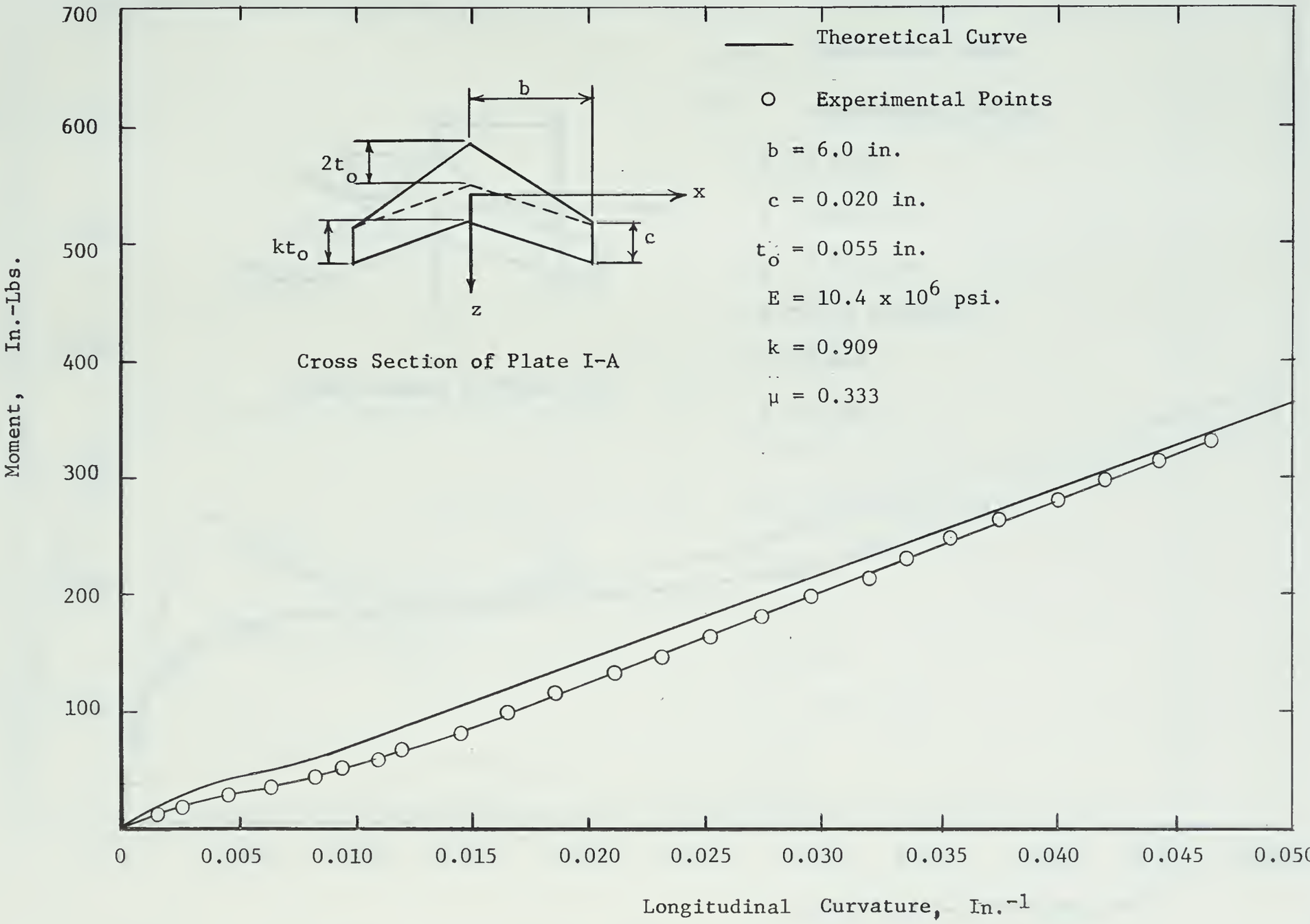

FIG. 3.2 COMPARISON OF THEORETICAL AND EXPERIMENTAL RESULTS FOR PLATE I-A

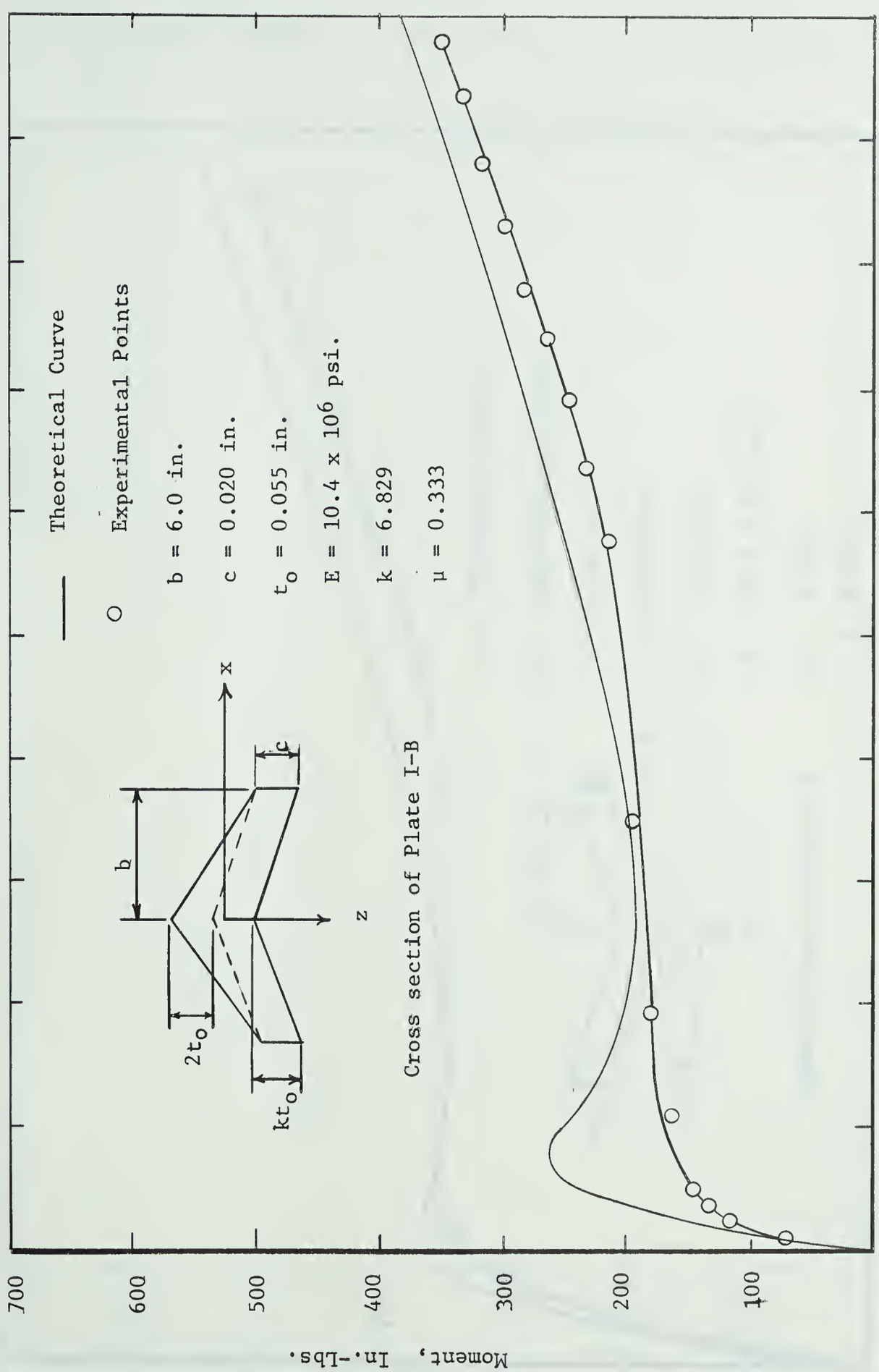

FIG. 3.3 COMPARISON OF THEORETICAL AND EXPERIMENTAL RESULTS FOR PLATE I-B

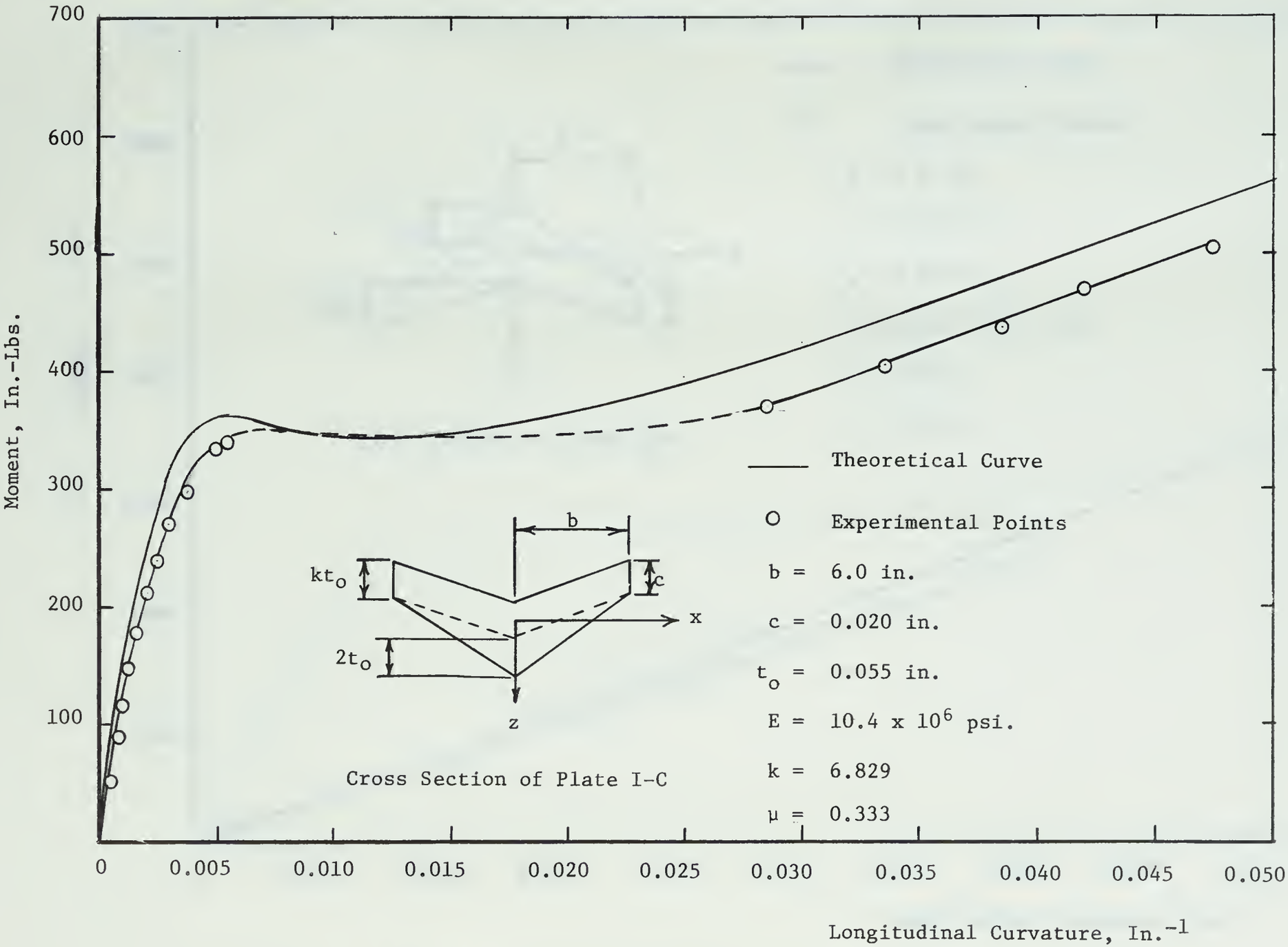

FIG. 3.4 COMPARISON OF THEORETICAL AND EXPERIMENTAL RESULTS FOR PLATE I-C

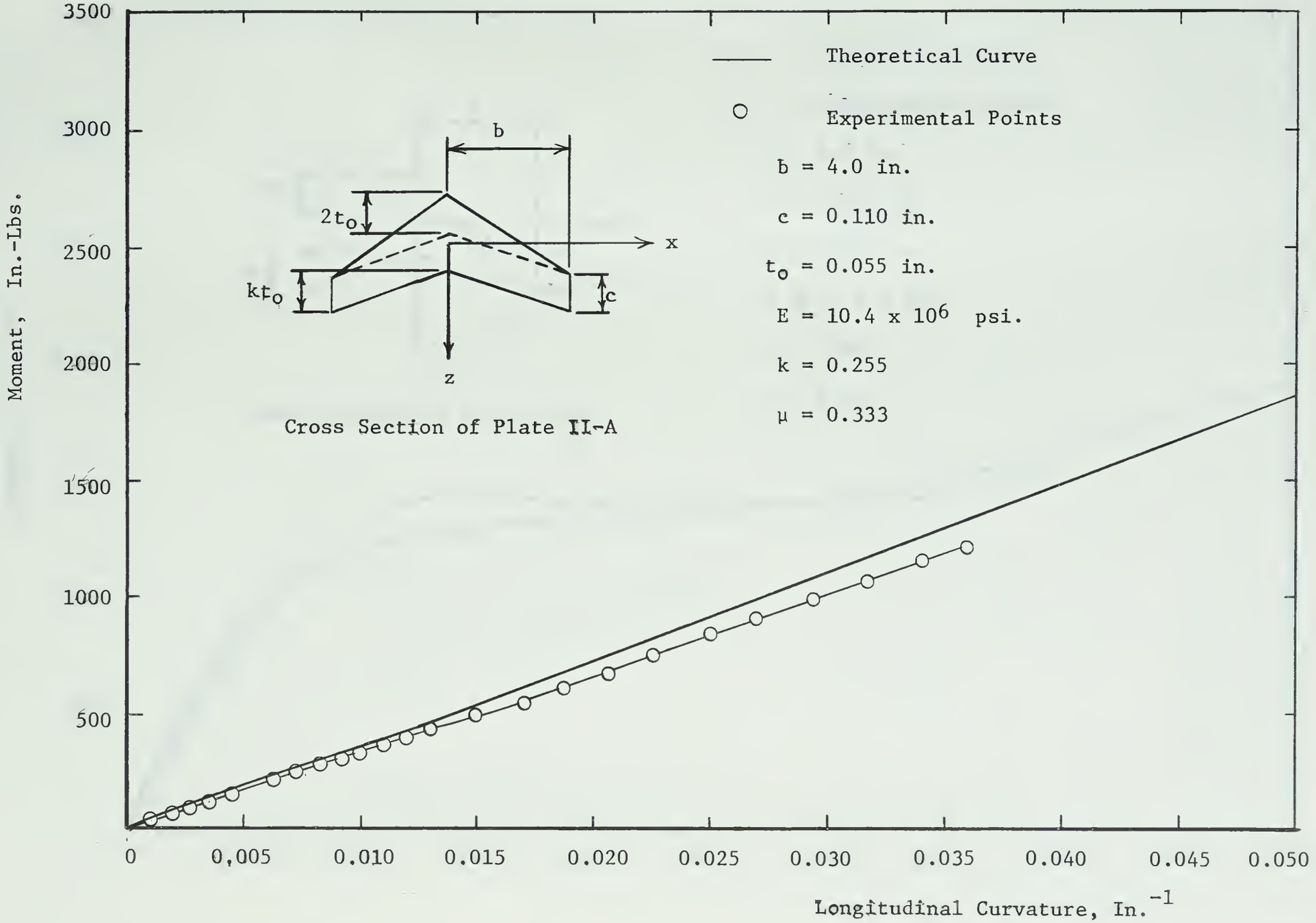

FIG 3.5 COMPARISON OF THEORETICAL AND EXPERIMENTAL RESULTS FOR PLATE II-A

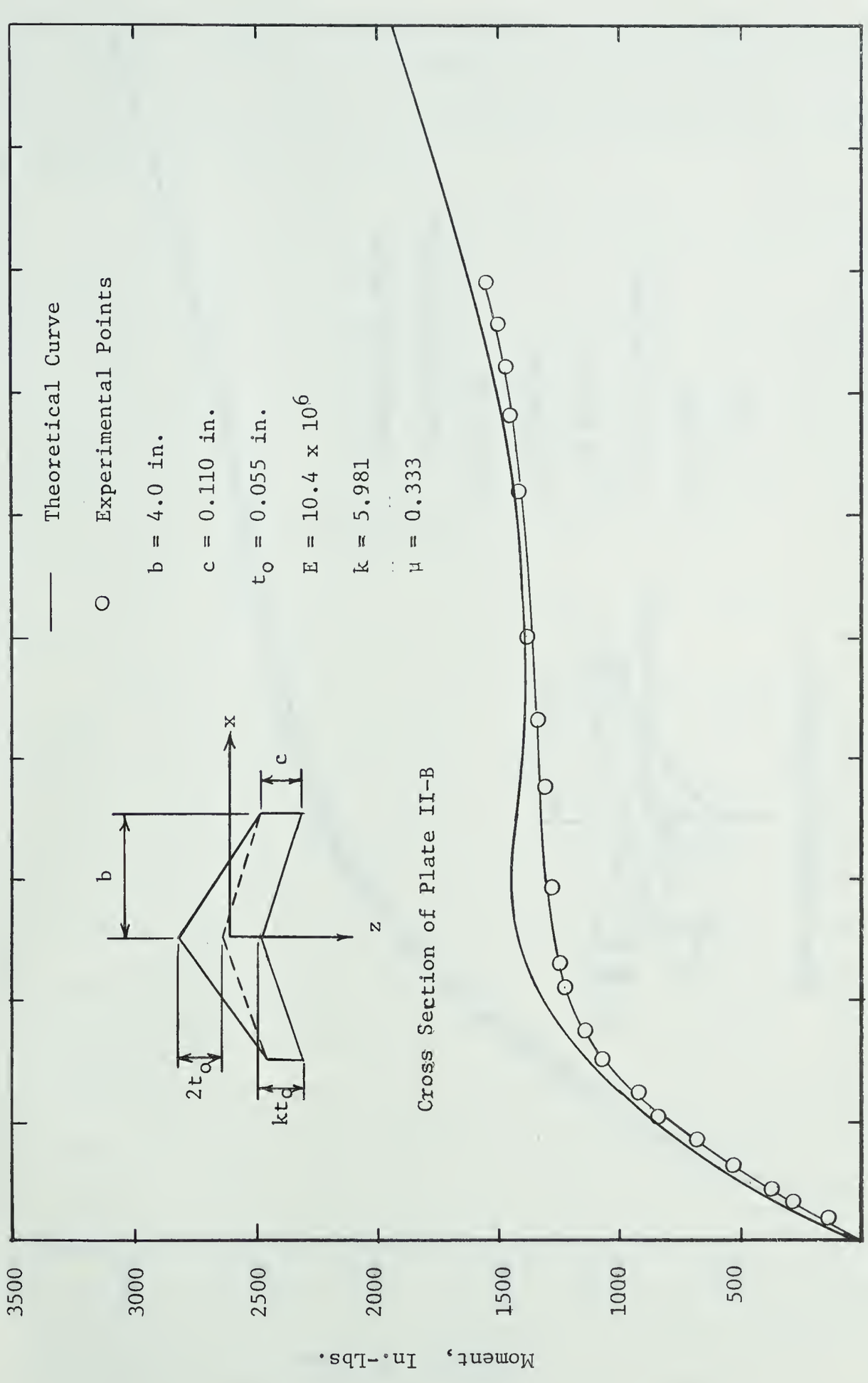

FIG. 3.6 COMPARISON OF THEORETICAL AND EXPERIMENTAL RESULTS FOR PLATE II-B

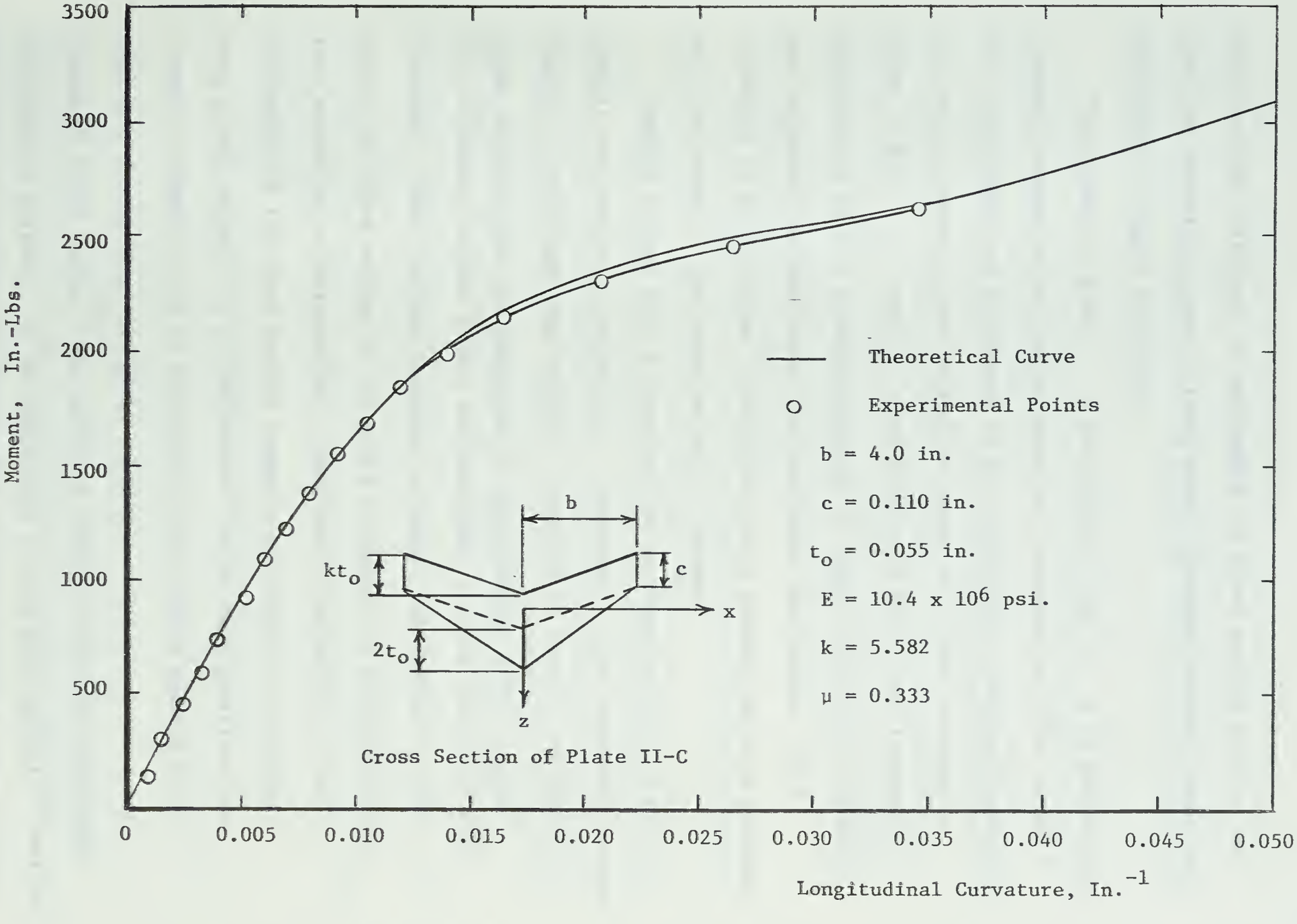

FIG 3.7 COMPARISON OF THEORETICAL AND EXPERIMENTAL RESULTS FOR PLATE II-C

cross section distorted, it approached the cross section used to obtain the theoretical curve, giving better agreement between theory and experiment at higher curvatures.

The curves for Plate I - B are shown in Fig. 3.3 A 38 percent discrepancy occured in the region where the curvature was 0.004 inches^{-1}. This discrepancy was attributed to the chacteristic torsional instability which occurred in the bending of plates with cross sections as shown in Fig. 3.3. When the cross section of the plate flattened out sufficiently so that torsional bending no longer dominated, reasonably good agreement between theory and experiment was reached. At a curvature of 0.029 inches^{-1}, the error was 14 percent and at a curvature of 0.049 inches^{-1}, the error was only 7 percent.

Bending a plate with a cross section as shown in Fig. 3.4 did not exhibit any torsional instability. Consequently, good agreement between theory and experiment was reached. According to theory, the plate becomes unstable when the curvature is approximately 0.0055 inches^{-1}. The difference between theory and experiment in this region was only 6 percent. When the next increment of moment was applied to the plate, the cross section of the plate flattened out instantaneously, thus exhibiting a characteristic condition of instability. The flattening of the cross section caused the curvature to increase from 0.0055 inches^{-1} to 0.0285 inches^{-1} before this additional increment of moment could be supported. After passing through this region of instability, the plate behaved more linearly. At a curvature of 0.050 inches^{-1} the agreement between theory and experiment was within 5 percent. It is interesting to note that Ashwell[4] verified his theory by carrying out experiments on steel measuring tapes, obtaining an error from 4 to 19 percent below that predicted by the theory.

Better agreement was reached for the Plate II series than for the Plate I series. Plate II - A (Fig. 3.5) showed an increase in the deviation between theoretical and experimental curves with increased curvature; however, the difference was only 8 percent at a curvature of 0.036 inches^{-1}. Plate II - B, Fig. 3.6, exhibited the same form of torsional instability as Plate I - B.

Fig. 3.7 for Plate II - C, showed excellent agreement between theory and experiment. This plate did not exhibit the bending instability characteristic shown by Plate I - C. Before this plate could exhibit bending instability, an increase in k would have to be made.

3.4 CONCLUDING REMARKS ON CHAPTER III

It was observed that for all six plates, the experimental moments were less than or equal to the theoretical moments at a particular curvature. One possible explanation for this was that the theoretical curves were based on the dimensions of the plate before the plate was bent into a longitudinal curvature. During the process of conducting three different tests on each plate, the plates gradually lost their camber; hence, reducing their stiffness and decreasing the moment required to bend them.

In addition to the errors caused by the non-linearity warping of the cross section and the inability to measure k accurately, other sources of error are:

(1) error in reading the strain gauges, and

(2) errors due to the frictional effects at the supports of the loading apparatus.

The error in reading the strain values was less than $\pm$ 5 percent, and the frictional error was approximately $\pm$ 2 percent. The total error due to the above causes was less than $\pm$7 percent.

CHAPTER IV

CONCLUSIONS AND FURTHER PROBLEMS

4.1 CONCLUSIONS

Theoretical and experimental investigations were described in this thesis for moment-curvature relationships of cambered bitrapezoidal plates. The theory presented was supported by experimental results. The general theory developed was shown to approach the previous theories for flat rectangular plates and for bitrapezoidal plates with no camber. In fact, the previous theories are special cases of the theory presented in this thesis.

In view of the good agreement obtained between theory and experiment and with previous theories for different cross sections, the theory can be expected to accurately predict the moment-curvature relationships for plates with cambered bitrapezoidal cross sections having an edge thickness.

4.2 PROBLEMS FOR FURTHER STUDY

In conducting experiments on the plates, it was observed that Plates I-B and II-B exhibited torsional instability. It would be interesting to investigate experimentally and theoretically the torsional instability of cambered bitrapezoidal plates.

Thus far, plates have been considered with linear thickness variations. The present theory could be extended to include thickness variations of second or higher order (i.e. semi-elliptic or semi-circular cross sections with camber).

TABLE OF REFERENCES

1. KELVIN, LORD and TAIT, P. G. Principle of Mechanics and Dynamics (formerly titled Treatise on Natural Philosphy) Dover Publications 1962, Part II, p. 266.

2. TIMOSHENKO, S. P. Collected Papers, McGraw-Hill, 1953, pp. 366-370.

3. FLÜGGE, W. "Large Deflections of Thin Wings", Technical Report No.3, Air Forces Contract W33-038 AC-16697, Stanford University, Stanford, California, 1949.

4. ASHWELL, D. G. "Characteristic Type of Instability in the Large Deflexions of Elastic Plates:
   I. Curved Rectangular Plates Bent About One Axis
   II. Flat Square Plates Bent About All Edges".
   Proceedings of the Royal Society, A, Vol. 214, 1952, pp. 98 - 109.

5. ASHWELL, D. G. "The Stability in Bending of Slightly Corrugated Plates", Journal of the Royal Aeronautical Society, Vol. 56, 1952, pp. 782 - 788.

6. FUNG, Y. C. and WITTRICK, W. H. "The Anticlastic Curvature of a Strip With Lateral Thickness Variation", Journal of Applied Mechanics, Vol. 21, 1954.

7. GOODIER, J. N. "Torsional and Flexural Buckling of Bars of Thin-Walled Open Section Under Compressive and Bending Loads", Journal of Applied Mechanics, Vol. 9, No. 3, September 1942, pp. A-103 to A-107.

8. LAMB, H. "On the Flexure of a Flat Elastic Spring", Philosophical Magazine, Series 5, Vol. 31, 1891, pp. 182 - 188.

9. BELLOW, D. G. and FAULKNER, M. G. "Bending Behaviour of a Rectangular Plate with a Bitrapezoidal Cross Section", Unpublished Paper.

10. FAULKNER, M. G. "Bending Behaviour of Bitrapezoidal Plates", Unpublished M.Sc. Thesis, University of Alberta, 1966.

11. TIMOSHENKO, S. P. and WOINOWSKY-KRIEGER, S. Theory of Plates and Shells, McGraw-Hill, 1959, pp. 488 - 497.

12. FLÜGGE, W. Stresses in Shells, Springer-Verlag, 1962, pp. 287-293.

13. ABRAMOWITZ, M. and STEGUN, I. A. Handbook of Mathematical Functions, AMS 55, National Bureau of Standards, 1965, pp. 379 - 385.

14. SEARLE, G. F. G. Experimental Elasticity, Cambridge University Press, 1908.

APPENDIX A

COMPUTER PROGRAM TO EVALUATE CONSTANTS OF INTEGRATION AND THEORETICAL MOMENT-CURVATURE RELATIONSHIPS

The following program consists of three parts: main program called "PLATE" and two subroutines called "SOLVE" and "BSL". First, the main program was used to solve for the order zero and one Bessel functions ber, bei, ker, and kei. By using various combinations of the order zero and one Bessel functions, the order two and the derivatives of the Bessel functions were calculated. A recursion formula was used to evaluate the above order zero and one functions, however, for arguments greater than ten, it was discovered that this recursion formula gave erroneous results for the ker and kei functions of order zero and one. Then subroutine "BSL" was added to the program so that whenever the argument, $\eta > 10$, this subroutine was called upon by the main program and the ker and kei functions of order zero and one were calculated using an asymptotic form of series. After the insertion of the "BSL" subroutine, the program computed the Bessel functions correctly.

After the necessary Bessel functions were computed, a 4 X 5 matrix was set up involving the four constants A, B, C, and D. Subroutine "SOLVE" was called upon to solve the matrix. The last part of the program is the calculation of moment-curvature relationship from Eqn. 1.3-11.

The program was initially written in single precision (i.e. using eight significant figures) however, it was soon discovered that due to computer "round-off" misleading results were obtained. The program was

then changed to double precision (i.e. using 16 significant figures) resulting in much improved results.

To facilitate in reading the computer program, some of the following symbols were used:

GAM	- γ, Euler's constant
YM	- E, Young's modulus
FMU	- μ, Poisson's ratio
TO	- t_o, amount of taper
FC	- c, edge thickness
FK1	- k, dimensionless parameter
FB	- b, one-half the plate width
BETA	- $\beta = \frac{c}{2t_o}$
FLA2, FLA4, etc.	- λ^2, λ^4, etc.
EP	- ε
AL	- α
ETA	- η
BR00	- ber η
BR10	- ber$'$ η
FKI11	- kei$_1'$ η
EBI02	- bei$_2$ ε
AKR01	- ker$_1$ α
X(1), X(2), X(3), X(4)	- A, B, C, D respectively
F1, ..., F26	- various parts of Eqn. 1.3-11
FM	- moment
R1	- 1/R, curvature.

The input data consisted of YM, FMU, TO, FC, FK1, and FB and the output was R1 and FM.

```
C     PROGRAM PLATE

C     COMPUTER PROGRAM FOR THE EVALUATION OF THEORETICAL MOMENT-
C     CURVATURE RELATIONSHIPS FOR PLATES WITH CAMBERED BITRAPEZOIDAL
C     CROSS SECTIONS
C
      COMMON A,X,FKR00,FKI00,FKR01,FKI01,ETA,N,NI
      DOUBLE PRECISION A(4,5),X(4),YM,FMU,T0,FC,FK1,FB,PI,GAM,FJ,FLA2,
     1FLA4,FLA8,FLA,BB,R,BETA,EP,AL,ETA,T,SUM,FI,SUM1,SUM2,B,C,PSI,FK,D,
     1PSI1,PSI2,A1,EP2,EP3,EP4,AL2,AL3,AL4,FMU2,T03,FM,FA,F1,F2,F3,F4,F5
     1,F6,F7,F8,F9,F10,F11,F12,F13,F14,F15,F16,F17,F18,F19,F20, F21,F22,
     1F23,F24,F25,F26,A23,B23,A24,B24,A25,B25,A26,B26,X12,X22,X32,X42,
     1 BI02,ABI02,EBI02,FKI02,EKI02,AKI02,X13,X24,X14,X23,R1,DL
      DOUBLE PRECISION
     1 BR00, BR10, BR20, BR01, BR11, BR02, BI00, BI10, BI20, BI01, BI11,
     1EBR00,EBR10,EBR20,EBR01,EBR11,EBR02,EBI00,EBI10,EBI20,EBI01,EBI11,
     1ABR00,ABR10,ABR20,ABR01,ABR11,ABR02,ABI00,ABI10,ABI20,ABI01,ABI11,
     1FKR00,FKR10,FKR20,FKR01,FKR11,FKR02,FKI00,FKI10,FKI20,FKI01,FKI11,
     1EKR00,EKR10,EKR20,EKR01,EKR11,EKR02,EKI00,EKI10,EKI20,EKI01,EKI11,
     1AKR00,AKR10,AKR20,AKR01,AKR11,AKR02,AKI00,AKI10,AKI20,AKI01,AKI11
  11  FORMAT(1HJ,1F13.4,1F13.1)
  27  FORMAT(6X,6D10.3)
      C=DSQRT(2D0)
      PI=3.1415926535897 9D0
      GAM=.5772156649015 3D0
      DO 28 JJ=1,25
      WRITE(6,29)
  29  FORMAT(1HK,5X,60H      YM         MU         TO         C          K
     1        B    )
      READ(5,27)YM,FMU,T0,FC,FK1,FB
      WRITE(6,27)YM,FMU,T0,FC,FK1,FB
      BETA=FC/(2D0*T0)
      BB=FB**2
      FMU2=FMU**2
      WRITE(6,26)
  26  FORMAT(1HL,26H    CURVATURE        MOMENT)
      DO 28 J=1,100,1
      FJ=J
      R1=.001D0*FJ
      R=1D0/R1
      FLA4=3D0*FB**4*(1D0-FMU2)/((T0*R)**2)
      FLA2=BB*DSQRT(3D0*(1D0-FMU2))/(R*T0)
      FLA=SQRT(FLA2)
      FLA8=FLA4**2
      EP=2D0*FLA*DSQRT(BETA)
      AL=2D0*FLA*DSQRT(1D0+BETA)
      ETA=EP
      L=1
C     BER ETA
  23  T=-(.25D0)**2*ETA**4/4D0
      SUM=1D0+T
      FI=1D0
```

```
C
C
C
C
C
```

```
    1 FI=FI+1D0
      T=-T*.25D0**2*ETA**4/((2D0*FI*(2D0*FI-1D0))**2)
      SUM=SUM+T
      IF(DABS(T).GE.5D-16) GO TO 1
      BR00=SUM
C     BEI ETA
      T=.25D0*ETA**2
      SUM=T
      FI=1D0
    3 FI=FI+1D0
      T=-T*(.25D0*ETA**2)**2/(((2D0*FI-1D0)*(2D0*FI-2D0))**2)
      SUM=SUM+T
      IF(DABS(T).GE.5D-16) GO TO 3
      BI00=SUM
C     BER AND BEI ETA FOR NU=1
      SUM1=DCOS(.75D0*PI)
      SUM2=DSIN(.75D0*PI)
      B=1.25D0
      FI=1D0
      T=.25D0*ETA**2/(FI*(FI+1D0))
      SUM1=SUM1+T*DCOS(B*PI)
      SUM2=SUM2+T*DSIN(B*PI)
    5 FI=FI+1D0
      B=B+.5D0
      T=T*.25D0*ETA**2/(FI*(FI+1D0))
      SUM1=SUM1+T*DCOS(B*PI)
      SUM2=SUM2+T*DSIN(B*PI)
      IF(DABS(T).GE.5D-16) GO TO 5
      BR01=.5D0*ETA*SUM1
      BI01=.5D0*ETA*SUM2
      BR10=(BR01+BI01)/C
      BI10=(BI01-BR01)/C
      BR20=-BI00-BR10/ETA
      BI20=BR00-BI10/ETA
      BR11=-(BR00+BI00)/C-BR01/ETA
      BI11=-(BI00-BR00)/C-BI01/ETA
      BR02=-C*(BR01-BI01)/ETA-BR00
      BI02=-C*(BI01+BR01)/ETA-BI00
C     KER ETA
      IF(ETA.LE.10D0) GO TO 31
      CALL BSL
      GO TO 30
   31 I=1
      DL=DLOG(.5D0*ETA)
      SUM=-GAM
      T=-(.25D0*ETA**2)**2/4D0
   15 I=I+1
      FI=I
      PSI=-GAM
      N=2*I-2
      DO 14 K=1,N
      FK=K
```

```
      FK=K
      DO 14 K=1,N
      N=2*I-2
      PSI=-GAM
      FI=I
   15 I=I+1
      T=-(.25D0*ETA**2)**2/4D0
      SUM=-GAM
      DL=DLOG(.5D0*ETA)
   31 I=1
      CALL BSL
      DO 1C 30
      IF(ETA.LE.1DD0) GO TO 31
C     KER ETA
      BI0=BR00-BI10/ETA
      BR20=-BI00-2BI0/ETA
      BR10=(BR01+BR00)/C
      BI10=(BI01-BR01)/C
      BR01=.5D0*ETA*SUM1
      BI01=.5D0*ETA*SUM2
      SUM2=SUM2+T*DCOS(B*PI)
      SUM1=SUM1+T*DCOS(B*PI)
      T=1.*.25D0*ETA**2/(FI*(FI+1DD))
      B=B+.5DD
    5 FI=FI+1DD
      SUM2=SUM2+T*DSIN(B*PI)
      SUM1=SUM1+T*DCOS(B*PI)
      T=.25D0*ETA**2/(FI*(FI+1DD))
      B=1.25DD
      FI=1DD
      IF(DABS(T).GE.5D-16) GO TO 5
      BI00=SUM2
      SUM2=DSIN(.75DD*PI)
      SUM1=DCOS(.75DD*PI)
C     BESR AND BEI ETA BIG ND=1
      T=-1*(.25D0*ETA**2)**2/(((2DD*FI-1DD)*(2DD*FI-2DD))*4.)
      SUM=SUM+T
      IF(DABS(T).GE.5D-16) GO TO 4
      BR00=SUM
      FI=FI+1DD
    3 FI=FI+1DD
      T=-1.*.25D0*ETA**2/(((2DD*FI-1DD)*(2DD*FI-2DD))*4.)
      SUM=SUM+T
      IF(DABS(T).GE.5D-16) GO TO 3
      PI00=SUM
      T=.5*SDD*ETA**2
      SUM=1
      FI=1DD
      T=-1.*.25D0*ETA**2
      SUM=SUM+T
      IF(DABS(T).GE.5D-16) GO TO 1
      PR00=SUM
C     BEI ETA
      DO 2 I=1,N
      T=-1.*.25D0*ETA**2/(FI*(FI+1DD))
      SUM=SUM+T*DCOS(B*PI)
      B=B+.5DD
      FI=FI+1DD
      IF(DABS(T).GE.5D-16) GO TO 2
      PI00=SUM
      BI00=PI00
      BR00=PR00
      DO 6 I=1,N
      FK=K
      T=-1.*.25D0*ETA**2/(FI*(FI+1DD))
      SUM=SUM+T*DCOS(B*PI)
      B=B+.5DD
      FI=FI+1DD
      IF(DABS(T).GE.5D-16) GO TO 6
      PI00=SUM
      SUM=SUM+1
      T=-1.*.25D0*ETA**2*(((2DD*FI-1.)*(2DD*FI-1DD))+4.)
    1 FI=FI+1DD
```

```
   14 PSI=PSI+1D0/FK
      D=T*PSI
      SUM=SUM+D
      T=-T*(.25D0*ETA**2)**2/((2D0*FI*(2D0*FI-1D0))**2)
      IF(DABS(D).GE.5D-16) GO TO 15
      FKR00=-DL*BR00+.25D0*PI*BI00+SUM
C     KEI ETA
      I=1
      SUM=(-GAM+1D0)*.25D0*ETA**2
      T=-(.25D0*ETA**2)**3/36D0
   16 I=I+2
      PSI=-GAM
      DO 17 K=1,I
      FK=K
   17 PSI=PSI+1D0/FK
      D=T*PSI
      SUM=SUM+D
      FI=I
      T=-T*(.25D0*ETA**2)**2/(((FI+2D0)*(FI+1D0))**2)
      IF(DABS(D).GE.5D-16) GO TO 16
      FKI00=-DL*BI00-.25D0*PI*BR00+SUM
C     KER1 AND KEI1 ETA
      I=1
      SUM1=DCOS(.75D0*PI)*(-2D0*GAM+1D0)
      SUM2=DSIN(.75D0*PI)*(-2D0*GAM+1D0)
      T=ETA**2/8D0
      B=1.25D0
   20 I=I+1
      FI=I
      N=I-1
      PSI1=-GAM
      DO 18 K=1,N
      FK=K
   18 PSI1=PSI1+1D0/FK
      PSI2=-GAM
      DO 19 K=1,I
      FK=K
   19 PSI2=PSI2+1D0/FK
      PSI=PSI1+PSI2
      A1=DSIN(B*PI)*PSI*T
      D=DCOS(B*PI)*PSI*T
      SUM1=SUM1+D
      SUM2=SUM2+A1
      T=T*.25D0*ETA**2/(FI*(FI+1D0))
      B=B+.5D0
      IF(DABS(D).GE.5D-16) GO TO 20
      FKR01=.25D0*ETA*SUM1+DCOS(.75D0*PI)/ETA-DL*BR01+.25D0*PI*BI01
      FKI01=.25D0*ETA*SUM2-DSIN(.75D0*PI)/ETA-DL*BI01-.25D0*PI*BR01
C     SOLVE FOR KER-KEI PRIME,KER-KEI 2PRIME,KER1-KEI1 PRIME,KER2-KEI2
   30 FKR10=(FKR01+FKI01)/C
      FKI10=(FKI01-FKR01)/C
      FKR20=-FKI00-FKR10/ETA
```

```
      PSI=PSI+100/FK
      D=I*PSI
      SUM=SUM+D
      T=-I*(.2500*ETA**2)**2/((2.0)**I*(2.0)*FI-100))*2)
      IF(ABS(D).GE.5E-16) GO TO 15
      FK100=-GL*8100-.2500*PI*8000+SUM
C     KERI AND KEII ETA
      I=1
      SUM1=LOG(.2500*PI)*(-200*GAM+100)
      SUM2=SIN(.2500*PI)*(-200*GAM+100)
      T=ETA**2/800
      B=1.2500
20    I=I+1
      FI=I
      N=I-1
      PSII=-GA*
      DO 18 K=1,N
      FK=K
18    PSII=PSII+100/FK
      PSI2=-GA*
      DO 19 K=1,I
      FK=K
19    PSI2=PSI2+100/FK
      PSI=PSII+PSI2
      A1=GSIN(B*PI)*PSI*I
      C=UCOS(B*PI)*PSI*T
      SUM1=SUM1+D
      SUM2=SUM2+BI
      T=T*.2500*ETA**2/(FI*(FI+100))
      B=B+.500
      IF(ABS(D).GE.5E-10) GO TO 20
      FKR01=.2500*ETA*SUM1+UCOS(.1500*PI)/ETA-01 *8R01+.2500*I*01
      FKI01=.2500*ETA*SUM2-USIN(.1500*PI)/ETA-01 *0101-.2500*I*
C     SOLVE FOR KER-KEI PSIE,KER-KEI 2201E,E-P1-KEI1 P100,
      FK110=(FKR01-FKI01)/C
      FK210=(FKR01+FKI01)/C
      FK210=-FK100-FK110/ETA
```

```
      FKI20=FKR00-FKI10/ETA
      FKR11=-(FKR00+FKI00)/C-FKR01/ETA
      FKI11=-(FKI00-FKR00)/C-FKI01/ETA
      FKR02=-C*(FKR01-FKI01)/ETA-FKR00
      FKI02=-C*(FKI01+FKR01)/ETA-FKI00
      IF(L.EQ.2)GO TO 25
      EBR00=BR00
      EBR10=BR10
      EBR20=BR20
      EBR01=BR01
      EBR11=BR11
      EBR02=BR02
      EBI00=BI00
      EBI10=BI10
      EBI20=BI20
      EBI01=BI01
      EBI11=BI11
      EBI02=BI02
      EKR00=FKR00
      EKR10=FKR10
      EKR20=FKR20
      EKR01=FKR01
      EKR11=FKR11
      EKR02=FKR02
      EKI00=FKI00
      EKI10=FKI10
      EKI20=FKI20
      EKI01=FKI01
      EKI11=FKI11
      EKI02=FKI02
      ETA=AL
      L=2
      GO TO 23
   25 ABR00=BR00
      ABR10=BR10
      ABR20=BR20
      ABR01=BR01
      ABR11=BR11
      ABR02=BR02
      ABI00=BI00
      ABI10=BI10
      ABI20=BI20
      ABI01=BI01
      ABI11=BI11
      ABI02=BI02
      AKR00=FKR00
      AKR10=FKR10
      AKR20=FKR20
      AKR01=FKR01
      AKR11=FKR11
      AKR02=FKR02
      AKI00=FKI00
```

```
      EI1=(EK100-EK110)/(2.*EL)
      EI2=-(EK100+EK110)/(2.*EL)
      EM11=-(EK100-EK110)/C-EK101/EL
      EM12=-C*(EK101-EK111)/EL-EK100
      EM21=-C*(EK101+EK111)/EL-EK110
      IF(L.EQ.2)GO TO 25
      BR00=BR00
      BR10=BR10
      BR20=BR20
      BR01=BR01
      BR11=BR11
      BR02=BR02
      BR100=BR00
      BR110=BR10
      BR120=BR20
      BR101=BR01
      BR111=BR11
      BR102=BR02
      EK00=EKR00
      EK10=EKR10
      EK20=EKR20
      EK01=EKR01
      EK11=EKR11
      EK02=EKR02
      EK100=EK100
      EK110=EK110
      EK120=EK120
      EK101=EK101
      EK111=EK111
      EK102=EK102
      EI=AL
      L=2
      GO TO 23
25    AMR00=BR00
      AMR10=BR10
      AMR20=BR20
      AMR01=BR01
      AMR11=BR11
      AMR02=BR02
      AMR100=BR00
      AMR110=BR10
      AMR120=BR20
      AMR101=BR01
      AMR111=BR11
      AMR102=BR02
      AKR00=EKR00
      AKR10=EKR10
      AKR20=EKR20
      AKR01=EKR01
      AKR11=EKR11
      AKR02=EKR02
      AKR100=EK100
```

```
AKI10=FKI10
AKI20=FKI20
AKI01=FKI01
AKI11=FKI11
AKI02=FKI02
EP2=EP**2
EP3=EP**3
EP4=EP**4
AL2=AL**2
AL3=AL**3
AL4=AL**4
A(1,1)=-EP3*EBR00-24D0*EP*EBI00-48D0*EBR10+8D0*EP2*EBI10
A(1,2)=-EP3*EBI00+24D0*EP*EBR00-48D0*EBI10-8D0*EP2*EBR10
A(1,3)=-EP3*EKR00-24D0*EP*EKI00-48D0*EKR10+8D0*EP2*EKI10
A(1,4)=-EP3*EKI00+24D0*EP*EKR00-48D0*EKI10-8D0*EP2*EKR10
A(1,5)=0D0
A(2,1)=-EP2*EBI10+4D0*EP*EBI00+8D0*EBR10
A(2,2)= EP2*EBR10-4D0*EP*EBR00+8D0*EBI10
A(2,3)=-EP2*EKI10+4D0*EP*EKI00+8D0*EKR10
A(2,4)= EP2*EKR10-4D0*EP*EKR00+8D0*EKI10
A(2,5)=FMU*BB*EP3*BETA/(R*FLA2)
A(3,1)=-2D0*ABR10-AL*ABI00
A(3,2)=-2D0*ABI10+AL*ABR00
A(3,3)=-2D0*AKR10-AL*AKI00
A(3,4)=-2D0*AKI10+AL*AKR00
A(3,5)=-T0*(1D0+FK1)*AL3/(2D0*FLA2)
A(4,1)=AL2*ABR00-2D0*AL*ABI10-EP2*EBR00+2D0*EP*EBI10
A(4,2)=AL2*ABI00+2D0*AL*ABR10-EP2*EBI00-2D0*EP*EBR10
A(4,3)=AL2*AKR00-2D0*AL*AKI10-EP2*EKR00+2D0*EP*EKI10
A(4,4)=AL2*AKI00+2D0*AL*AKR10-EP2*EKI00-2D0*EP*EKR10
A(4,5)=-6D0*FMU*BB/(4D0*R*FLA4)*(AL4-EP4)
N=4
CALL SOLVE
T03=T0**3
FM=YM*FB*T03/((1D0-FMU2)*768D0*FLA8*R)*(EP**8-AL**8)
FA=YM*FMU*T03/((12D0*FB*FLA4)*(1D0-FMU2))
F1=(EP2*EBR00-2D0*EP*EBI10-AL2*ABR00+2D0*AL*ABI10)*X(1)
F2=(EP2*EBI00+2D0*EP*EBR10-AL2*ABI00-2D0*AL*ABR10)*X(2)
F3=(EP2*EKR00-2D0*EP*EKI10-AL2*AKR00+2D0*AL*AKI10)*X(3)
F4=(EP2*EKI00+2D0*EP*EKR10-AL2*AKI00-2D0*AL*AKR10)*X(4)
F5=-(EP3*EBR10-AL3*ABR10)*X(1)+3D0*F1
F6=-(EP3*EBI10-AL3*ABI10)*X(2)+3D0*F2
F7=-(EP3*EKR10-AL3*AKR10)*X(3)+3D0*F3
F8=-(EP3*EKI10-AL3*AKI10)*X(4)+3D0*F4
FM=FM+FA*3D0/2D0*(F1+F2+F3+F4+F5+F6+F7+F8)
F 9=(EP4*EBR20-AL4*ABR20)*X(1)+4D0*F5
F10=(EP4*EBI20-AL4*ABI20)*X(2)+4D0*F6
F11=(EP4*EKR20-AL4*AKR20)*X(3)+4D0*F7
F12=(EP4*EKI20-AL4*AKI20)*X(4)+4D0*F8
FM=FM+FA*.5D0*(F9+F10+F11+F12)
FM=FM+9D0*YM*FMU2*FB**5*T0/(2D0*R**3*FLA2**6)*(EP4-AL4)
F13=F1
```

```
      SUBROUTINE SOLVE
      DIMENSION A(4,5),B(4),X(4)
      N=4
      DO 1 K=1,N
      DO 2 I=K,N
      IF(ABS(A(I,K)).GT.ABS(A(K,K))) GO TO 3
      GO TO 2
    3 DO 4 J=K,5
      T=A(K,J)
      A(K,J)=A(I,J)
      A(I,J)=T
    4 CONTINUE
    2 CONTINUE
      DO 5 I=K+1,N
      DO 6 J=K+1,5
      A(I,J)=A(I,J)-A(I,K)*A(K,J)/A(K,K)
    6 CONTINUE
    5 CONTINUE
    1 CONTINUE
      X(N)=A(N,5)/A(N,N)
      DO 7 I=1,N-1
      K=N-I
      S=0.0
      DO 8 J=K+1,N
      S=S+A(K,J)*X(J)
    8 CONTINUE
      X(K)=(A(K,5)-S)/A(K,K)
    7 CONTINUE
      DO 9 I=1,N
      B(I)=X(I)
    9 CONTINUE
      RETURN
      END
```

```
      F14=F2
      F15=F3
      F16=F4
      FM=FM-6D0*YM*FMU*FB**3*T0/(R**2*FLA8)*(F13+F14+F15+F16)
      X12=X(1)**2
      X22=X(2)**2
      F17=(X12+X22)*(EP*(EBR01*EBI11-EBR11*EBI01)-AL*(ABR01*ABI11-ABR11*
     1ABI01))
      F18=(X12-X22)*(EP2*(2D0*EBR01*EBI01-EBR00*EBI02-EBR02*EBI00)-AL2*(
     12D0*ABR01*ABI01-ABR00*ABI02-ABR02*ABI00))/2D0
      X32=X(3)**2
      X42=X(4)**2
      F19=(X32+X42)*(EP*(EKR01*EKI11-EKR11*EKI01)-AL*(AKR01*AKI11-AKR11*
     1AKI01))
      F20=(X32-X42)*(EP2*(2D0*EKR01*EKI01-EKR00*EKI02-EKR02*EKI00)-AL2*(
     12D0*AKR01*AKI01-AKR00*AKI02-AKR02*AKI00))/2D0
      F21=-X(1)*X(2)*(EP2*(EBR01**2-EBR00*EBR02-EBI01**2+EBI00*EBI02)-AL
     12*(ABR01**2-ABR00*ABR02-ABI01**2+ABI00*ABI02))
      F22=-X(3)*X(4)*(EP2*(EKR01**2-EKR00*EKR02-EKI01**2+EKI00*EKI02)-AL
     12*(AKR01**2-AKR00*AKR02-AKI01**2+AKI00*AKI02))
      A23=EP2*(2D0*EBR01*EKI01-EBR00*EKI02-EBR02*EKI00+2D0*EBI01*EKR01-E
     1BI00*EKR02-EBI02*EKR00)
      B23=AL2*(2D0*ABR01*AKI01-ABR00*AKI02-ABR02*AKI00+2D0*ABI01*AKR01-A
     1BI00*AKR02-ABI02*AKR00)
      X13=X(1)*X(3)
      X24=X(2)*X(4)
      F23=(X13-X24)/2D0*(A23-B23)
      A24=-EP*(EBR11*EKI01-EBR01*EKI11-EBI11*EKR01+EBI01*EKR11)
      B24=-AL*(ABR11*AKI01-ABR01*AKI11-ABI11*AKR01+ABI01*AKR11)
      F24=(X13+X24)*(A24-B24)
      X14=X(1)*X(4)
      X23=X(2)*X(3)
      A25=EP2*(-2D0*EBR01*EKR01+EBR00*EKR02+EBR02*EKR00+2D0*EBI01*EKI01-
     1EBI00*EKI02-EBI02*EKI00)
      B25=AL2*(-2D0*ABR01*AKR01+ABR00*AKR02+ABR02*AKR00+2D0*ABI01*AKI01-
     1ABI00*AKI02-ABI02*AKI00)
      F25=(X14+X23)/2D0*(A25-B25)
      A26=EP*(EBR11*EKR01-EBR01*EKR11+EBI11*EKI01-EBI01*EKI11)
      B26=AL*(ABR11*AKR01-ABR01*AKR11+ABI11*AKI01-ABI01*AKI11)
      F26=(X14-X23)*(A26-B26)
      FM=FM+YM*FB*T0/(4D0*R*FLA4)*(F17+F18+F19+F20+F21+F22+F23+F24+F25+F
     126)
   28 WRITE(6,11) R1,FM
      STOP
      END
```

```
      STOP
      END
```

```
      SUBROUTINE SOLVE

      COMMON A,X,FKR00,FKI00,FKR01,FKI01,ETA,N,NI
      DOUBLE PRECISION A(4,5),X(4),FKR00,FKI00,FKR01,FKI01,ETA,AMAX,TS,
     1FMULTP,FNUM
      M=N+1
      NM1=N-1
      DO 100 I=1,N
  100 A(I,M)=-A(I,M)
      DO 101 I=1,NM1
      AMAX=A(I,I)
      K=I
      DO 102 J=I,N
      IF(DABS(A(J,I)).LE.DABS(AMAX)) GO TO 102
      AMAX=A(J,I)
      K=J
  102 CONTINUE
      IF(AMAX.NE.0.0)GO TO 103
      RETURN
  103 IF(DABS(AMAX).GE.1D-21) GO TO 104
      WRITE(6,105)
  105 FORMAT(1HJ,14X,45H MATRIX IS EITHER SINGULAR OR ILL CONDITIONED)
  104 DO 106 J=I,M
      TS=A(I,J)
      A(I,J)=A(K,J)
  106 A(K,J)=TS
      IP1=I+1
      DO 107 J=IP1,N
      FMULTP=A(J,I)/A(I,I)
      DO 107 L=IP1,M
  107 A(J,L)=A(J,L)-FMULTP*A(I,L)
  101 CONTINUE
      X(N)=A(N,M)/A(N,N)
      DO 108 I=1,NM1
      K=N-I
      KP1=K+1
      FNUM=0D0
      DO 109 J=KP1,N
  109 FNUM=FNUM+X(J)*A(K,J)
  108 X(K)=(A(K,M)-FNUM)/A(K,K)
      RETURN
      END
```

```
      SUBROUTINE SOLVE
C
      COMMON A,X,IRANGE,ERR100,ERR=01,ERR101,ETA,P,II
      DOUBLE PRECISION A(II,II),X(I),ERR100,ERR101,ETA,P,TEMP
      IF(NULTP.EQ.0
      N=N+1
      NM1=N-1
      DO 100 I=1,N
  100 A(I,P)=-A(I,N)
      DO 101 I=1,NM1
      AMAX=A(I,I)
      K=I
      DO 102 J=I,N
      IF(DABS(A(J,I)).LE.DABS(AMAX)) GO TO 102
      AMAX=A(J,I)
      K=J
  102 CONTINUE
      IF(AMAX.NE.0.0)GO TO 103
      RETURN
  103 IF(DABS(AMAX).GE.1D-21) GO TO 104
      WRITE(6,105)
  105 FORMAT(1H0,14X,45H MATRIX IS EITHER SINGULAR OR ILL CONDITION
  104 DO 106 J=I,N
      TS=A(I,J)
      A(I,J)=A(K,J)
  106 A(K,J)=TS
      IP1=I+1
      DO 107 J=IP1,N
      FMULTP=A(J,I)/A(I,I)
      DO 107 L=IP1,M
  107 A(J,L)=A(J,L)-FMULTP*A(I,L)
  101 CONTINUE
      X(N)=A(N,M)/A(N,N)
      DO 108 I=1,NM1
      K=N-I
      KP1=K+1
      FNUM=0.0
      DO 109 J=KP1,N
  109 FNUM=FNUM+X(J)*A(K,J)
  108 X(K)=(A(K,M)-FNUM)/A(K,K)
      RETURN
      END
```

```
      SUBROUTINE BSL
C     ASSYMPTOTIC EXPANSION OF KER KEI KER1 KEI1
C
      COMMON A,X,FKR00,FKI00,FKR01,FKI01,ETA,N,NI
      DOUBLE PRECISION A(4,5),X(4),FKR00,FKI00,FKR01,FKI01,ETA,S2,SUM1,S
     1UM2,PI,BETA,FC,C,S,B,T,FI
      S2=DSQRT(2D0)
      PI=3.1415926535897D0
      SUM1=1D0
      SUM2=0D0
      BETA=ETA/S2+PI/8D0
      FC=DSQRT(PI/(2D0*ETA))*DEXP(-ETA/S2)
      B=.25D0
      I=1
      JC=2
      JS=4
      JCP=4
      JSP=2
      JCCP=8
      JSSP=6
      T=-1D0/(8D0*ETA)
      SUM1=SUM1+T*DCOS(PI*B)
      SUM2=SUM2+T*DSIN(PI*B)
    3 I=I+1
      FI=I
      B=B+.25D0
      IF(I.EQ.JC) GO TO 4
      IF(I.EQ.JCP) GO TO 22
      IF(I.EQ.JCCP) GO TO 23
      C=DCOS(PI*B)
      GO TO 5
    4 C=0D0
      JC=JC+4
      T=T*(-(2D0*FI-1D0)**2)/(FI*8D0*ETA)
      GO TO 18
   22 C=-1D0
      JCP=JCP+8
      GO TO 5
   23 C= 1D0
      JCCP=JCCP+8
    5 T=T*(-(2D0*FI-1D0)**2)/(FI*8D0*ETA)
      SUM1=SUM1+T*C
   18 IF(I.EQ.JS) GO TO 6
      IF(I.EQ.JSP) GO TO 24
      IF(I.EQ.JSSP) GO TO 25
      S=DSIN(PI*B)
      GO TO 7
    6 S=0D0
      JS=JS+4
      GO TO 19
```

```
      SUBROUTINE
C
C     ASSYMPTOTIC EXPANSION OF KEI KEI1
C
      COMMON A,X,PRECIS,FACTOR,ETA,PI,
     1 PRECISION A(4,3),X(4),TKR00,TKI00,TKR01,TKI01,FACTOR,
     2 IUM2,PI,BETA,FC,C,S,T,FI
      S2=SQRT(2D0)
      PI=3.14159265358979D0
      SUM1=1D0
      SUM2=0D0
      BETA=ETA/S2+PI/8D0
      FC=SQRT(PI/(2D0*ETA))*DEXP(-ETA/S2)
      B=.25D0
      I=1
      JC=2
      J2=4
      JCP=4
      J2P=2
      JCCP=6
      J2PP=8
      T=-1D0/(8D0*ETA)
      SUM1=SUM1+T*DCOS(PI*B)
      SUM2=SUM2+T*DSIN(PI*B)
    3 I=I+1
      FI=I
      B=B+.25D0
      IF(I.EQ.JC) GO TO 4
      IF(I.EQ.JCP) GO TO 22
      IF(I.EQ.JCCP) GO TO 23
      C=DCOS(PI*B)
      GO TO 5
    4 C=0D0
      JC=JC+4
      T=T*(-(2D0*FI-1D0)**2)/(FI*8D0*ETA)
      GO TO 10
   22 C=-1D0
      JCP=JCP+8
      GO TO 5
   23 C= 1D0
      JCCP=JCCP+8
    5 T=T*(-(2D0*FI-1D0)**2)/(FI*8D0*ETA)
      SUM1=SUM1+T*C
   10 IF(I.EQ.J2) GO TO 6
      IF(I.EQ.J2P) GO TO 24
      IF(I.EQ.J2PP) GO TO 25
      S=DSIN(PI*B)
      GO TO 7
    6 S=0D0
      J2=J2+4
      GO TO 19
```

```
24 S=1D0
   JSP=JSP+8
   GO TO 7
25 S=-1D0
   JSSP=JSSP+8
 7 SUM2=SUM2+T*S
19 IF(DABS(T).GE.1D-08) GO TO 3
   C=DCOS(BETA)
   S=DSIN(BETA)
   FKR00=FC*(SUM1*C-SUM2*S)
   FKI00=FC*(-SUM1*S-SUM2*C)
   I=1
   JC=2
   JS=4
   JCP=4
   JSP=2
   JCCP=8
   JSSP=6
   SUM1=1D0
   SUM2=0D0
   B=.25D0
   T=3D0/(8D0*ETA)
   BETA=ETA/S2+.625D0*PI
   SUM1=SUM1+T*DCOS(PI*B)
   SUM2=SUM2+T*DSIN(PI*B)
12 I=I+1
   FI=I
   B=B+.25D0
   IF(I.EQ.JC) GO TO 8
   IF(I.EQ.JCP) GO TO 26
   IF(I.EQ.JCCP) GO TO 27
   C=DCOS(PI*B)
   GO TO 9
 8 C=0D0
   JC=JC+4
   T=T*(4D0-(2D0*FI-1D0)**2)/(FI*8D0*ETA)
   GO TO 20
26 C=-1D0
   JCP=JCP+8
   GO TO 9
27 C=1D0
   JCCP=JCCP+8
 9 T=T*(4D0-(2D0*FI-1D0)**2)/(FI*8D0*ETA)
   SUM1=SUM1+T*C
20 IF(I.EQ.JS) GO TO 10
   IF(I.EQ.JSP) GO TO 28
   IF(I.EQ.JSSP) GO TO 29
   S=DSIN(PI*B)
   GO TO 11
10 S=0D0
   JS=JS+4
   GO TO 21
```

```
      J=1
      JC=2
      JS=4
      JCP=4
      JSP=2
      JCCP=8
      JSSP=16
      SUM1=100.
      SUM2=000.
      P=.25000
      T=300./(400.*PI*A)
      BETA=PI*A/2.+.625E0*P1
      SUM1=SUM1+T*COS(PI*B)
      SUM2=SUM2+T*SIN(PI*B)
   12 I=I+1
      PI=I
      B=B+.25E0
      IF(I.EQ.JC) GO TO 8
      IF(I.EQ.JCP) GO TO 26
      IF(I.EQ.JCCP) GO TO 27
      C=COS(PI*B)
      GO TO 9
    8 C=000.
      JC=JC+4
      T=T*(4.E0-(2.E0*PI-1.E0)**2)/(PI*BETA)
      GO TO 20
   26 C=-1.E0
      JCP=JCP+8
      GO TO 9
   27 C=1.E0
      JCCP=JCCP+8
    9 T=T*(4.E0-(2.E0*PI-1.E0)**2)/(PI*BETA)
      SUM1=SUM1+T*C
   20 IF(I.EQ.JS) GO TO 10
      IF(I.EQ.JSP) GO TO 28
      IF(I.EQ.JSSP) GO TO 29
      S=SIN(PI*B)
      GO TO 11
   10 S=0.E0
      JS=JS+4
      GO TO 21
```

```
28 S=1D0
   JSP=JSP+8
   GO TO 11
29 S=-1D0
   JSSP=JSSP+8
11 SUM2=SUM2+T*S
21 IF(DABS(T).GE.1D-08) GO TO 12
   C=DCOS(BETA)
   S=DSIN(BETA)
   FKR01=FC*(SUM1*C-SUM2*S)
   FKI01=FC*(-SUM1*S-SUM2*C)
   RETURN
   END
```

```
      S=SIN(
      JSP=JS*
      DO 11
      S=-1.0
      JSP=JS*S+
11    SUM2=SUM2+T*S
      IF(DABS(T).GE.1.D-
      C=DCOS(BETA)
      S=DSIN(BETA)
      FNRO1=FC*(SUM1*C-SUM2*S)
      FR101=FC*(-SUM1*S-SUM2*C)
      RETURN
      END
```

APPENDIX B

COMPUTER PROGRAM FOR EVALUATING BENDING MOMENT AND LONGITUDINAL CURVATURE FROM STRAIN GAUGE READINGS

The program shown below determined the curvature using Eqn. 2.4-2. The particular program shown is for Plate II-C. The program was applicable to all the plates tested after the appropriate changes were made to it. The input data used was the double bending strain e_B. After the radius of curvature, R, was calculated, the program determined the correction moment, M_1, using Eqn. 3.2-1. The correction moment was then subtracted from the applied moment, yielding the correct value for the moment. Output consists of e_B and the corresponding support distance, applied load, arc length from mid-line to measuring station under consideration, correction moment, curvature and moment. For ease in reading the program the following symbols were used:

W	- weight per unit length of plate
SUPD or A	- one-half the distance between the end supports of the plate
THNS	- distance between strain gauges at a particular measuring station (i.e. thickness of plate at centerline)
S	- distance from mid-line to measuring station measured along the plate
FL	- applied load to pulley rims
E (L) or ET - EB	- e_B
FM	- moment
Y	- P, horizontal distance from mid-line to measuring station
FM1 or M1	- M_1, correction moment
R1	- 1/R, curvature

The symbols not defined above are self-explanatory in the program.

```
C      COMPUTER PROGRAM FOR THE EVALUTION OF EXPERIMENTAL RESULTS FOR
C      PLATE II-C
C
       W=.1333
       SUPD=16.75
       THNS=.221
     1 FORMAT(1X,14I5)
     2 FORMAT(1X,7F10.3)
     3 FORMAT(1HJ,4F10.2,2F10.4,1F10.1)
       DIMENSION J(340),E(340)
       DO 6 I=1,5
       READ(5,2) S
       WRITE(6,5)
     5 FORMAT(1HK,70H  ET-EB     SUP DIST      LOAD         ARC           M1
      1      1/R    MOMENT )
       READ(5,1) (J(K), K=20,340,20)
       DO 6 L=20,340,20
       FL=L
       E(L)=J(L)
       FM=7.625*FL
       R=THNS/(E(L)*1.E-06)
       TH=S/ABS(R)
       Y=ABS(R)*SIN(TH)
       A=ABS(R)*SIN(SUPD/ABS(R))
       FM1=-W*SUPD*(A-Y)-W*ABS(R)*(SQRT(R*R-A*A)-SQRT(R*R-Y*Y)+Y*(SUPD/AB
      1S(R)-TH))
       FM=FM+FM1
       R1=1./R
     6 WRITE(6,3) E(L),A,FL,S,FM1,R1,FM
       STOP
       END
```

```
C
C
C
```